NOTE TO USERS

uOttawa

L'Université canadienne
Canada's university

FACULTÉ DES ÉTUDES SUPÉRIEURES ET POSTOCTORALES

uOttawa

L'Université canadienne
Canada's university

FACULTY OF GRADUATE AND POSDOCTORAL STUDIES

Chuan Yu

AUTEUR DE LA THESE / AUTHOR OF THESIS

M.Sc. (Microbiology and Immunology spec. Human and Molecular Genetics)

GRADE / DEGREE

Department of Biochemistry, Microbiology and Immunology

FACULTÉ, ÉCOLE, DÉPARTEMENT / FACULTY, SCHOOL, DEPARTMENT

Mouse retinal histogenesis in the context of cell autonomous Hedgehog signalling pathway activation

TITRE DE LA THÈSE / TITLE OF THESIS

Valerie Wallace

DIRECTEUR (DIRECTRICE) DE LA THÈSE / THESIS SUPERVISOR

CO-DIRECTEUR (CO-DIRECTRICE) DE LA THÈSE / THESIS CO-SUPERVISOR

EXAMINATEURS (EXAMINATRICES) DE LA THÈSE / THESIS EXAMINERS

Marie-Andree Akimenko

Ilona Skerjanc

Gary W. Slater

LE DOYEN DE LA FACULTÉ DES ÉTUDES SUPÉRIEURES ET POSTDOCTORALES /
DEAN OF THE FACULTY OF GRADUATE AND POSTDOCORAL STUDIES

Mouse retinal histogenesis in the context of cell autonomous Hedgehog signalling pathway activation

by

Chuan Yu

Thesis submitted to the
Faculty of Graduate and Postdoctoral Studies
In partial fulfillment of the requirements
For the M.Sc. degree in the specialization of Human and Molecular Genetics

Department of Biochemistry, Microbiology and Immunology
Faculty of Medicine
University of Ottawa

Your file Votre référence
ISBN: 0-494-11468-1
Our file Notre référence
ISBN: 0-494-11468-1

Abstract

The adult mouse retina is a laminated assemblage of specialized neurons and glia, which serves as a model system for cell type specification in the CNS (central nervous system). The multiple cell types in the retina are derived from a retinal neuroepithelium, which contains multipotent retinal precursor cells (RPCs) that differentiate into specific retinal cell types. The morphogen Shh is expressed in the retinal ganglion cells (RGCs), and signals to the RPCs located in the overlying neuroblast layer of the developing retina. To distinguish between cell- and non-cell autonomous effects of the Hh signalling pathway activation in the RPCs, I have examined the effects of constitutive cell-autonomous activation of the Hh signalling pathway in the RPCs. The results showed that it promoted proliferation of RPCs and differentiation of the INL (inner nuclear layer) cells in a cell-autonomous way, and also affected the rod photoreceptor differentiation in a non-cell autonomous way.

Acknowledgements

First and foremost, my heartfelt gratitude goes to my adviser, Dr. Valerie Wallace. From the day Valerie introduced me to Canada and the field of retinal development, I was intrigued. During my stay at her lab, her relentless pursuit for the truth in science impressed me much that I could feel guilty, sometimes, for not continuing my studies. Furthermore, her patience to my progress and my thesis writing revision inspired my devotion to perfecting what I was doing, and will, for sure, affect my life in the future.

Sincere thanks also go to my Thesis Advisory Committee members, Dr. David Picketts and Dr. Catherine Tsilfidis, for their good suggestions and care for my project.

The colleagues in the Wallace lab are very nice to send out help, most of all; Dr. Yaping Wang helped me a lot with the retinal explant cultures; Dr. Gabriel Dakubo and Dr. Marosh Furimsky answered many of my questions and helped me out of the messy contexts; Ms. Chantal Mazerolle and Ms. Sherry Thurig supplemented a lot of stuff for the whole lab; Ms. Dana Wall, Ms. Hong Liu and Mr. Shawn Beug gave me much encouragement. I just enjoyed every moment in the lab and wish I could share the happiness brought up by the next Christmas door decoration.

I will miss all of you much when I am back to China.

To my friends back home in Mainland China, your emails were like lifelines, bridging the distance across the seas and the continents, pulling me closer.

Last and most importantly, my deepest thanks go to my family, Dad, Mum and Sister with her families, for always giving me their love. Finally, to my husband Mr. Jianxue Gao, who listened to my grumbles all these years, including the period before the marriage, shared the every exciting moment with me, and for always being there.

Table of Contents

List of Abbreviations

Amp	amphotropic
BCIP	5-Bromo-4-chloro-3-indolyl-phosphate
bFGF	basic fibroblast growth factor
bHLH	basic helix-loop-helix
BMP	bone morphogenetic protein
BrdU	bromodeoxyuridine
C3H 10T1/2 cell	mouse osteoblast cell line
CDK	Cyclin-dependent kinase
CFU	colony-forming units
CGNPs	cerebellar granule neuron precursors
CKIs	Cyclin-kinase inhibitor proteins
Chx 10	Ceh-10 homeodomain containing homolog
Ci	Cubitus interruptus
CNS	central nervous system
CNTF	ciliary neurotrophic factor
CRX	cone-rod homeobox
Dach	a homologue of Drosophila dachshund
Dhh	Desert Hedgehog
Dpp	decapentaplegic
ECM	extracellular matrix
Eco	ecotropic
EGF	epidermal growth factor
ERK	extracellular signal-regulated kinase

env	envelope gene of retrovirus
FCS	fetal calf serum
FGF	fibroblast growth factor
Fu	Fused
gag	structural genes of retrovirus
GCL	ganglion cell layer
eGFP	enhanced green fluorescent protein
GFAP	glial fibrillary acidic protein
GPCR	G-protein coupled receptor
Hh	Hedgehog
Ihh	Indian Hedgehog
IGF	insulin-like growth factor
IRES	internal ribosome entry site
INL	inner nuclear layer
IPL	inner plexiform layer
Kip	kinase inhibitor protein
MEFs	mouse embryonic fibroblasts
min	minute(s)
NBT	4-Nitro blue tetrazolium chloride
ONL	outer nuclear layer
OPL	outer plexiform layer
Optx	electronic chart information
NIH 3T3 cell	mouse fibroblast cell line
PBS	phosphate buffered saline

PFA	paraformaldehyde
Phoenix-Eco cell	packaging cell line based on the 293T cell line
pol	reverse transcriptase of retrovirus
Ptc	Patched
PVA	polyvinyl alcohol
Rb	retinoblastoma
RGC	retina ganglion cell
RPC	retinal pecursor cell
RPE	retina pigment epithelium
RT	room temperature
RTK	receptor tyrosine kinase
RT-PCR	reverse transcription-polymerase chain reaction
SCF	stem cell factor
Shh	Sonic Hedgehog
Smo	Smoothened
Syu	sonic you
Su(fu)	Suppressor of fused
TGF	transforming growth factor
TGFα	transforming growth factor α
TF	transcription factor
ZPA	zone of polarizing activity

List of Figures

List of Tables

Still round the corner there may wait,

a new road or a secret gate.

- J. R. R. Tolkien

Introduction

1.1 Development of the mouse retina

Along with the brain and the spinal cord, the retina is one part of the central nervous system (CNS). In mice, eyes first appear as outgrowths, optic vesicles, emanating from the ventral diencephalon at embryonic day 8.5 (E8.5). The optic vesicles grow laterally, contact the surface ectoderm, induce the formation of a lens placode and invaginate, such that by E10.5, the developing eye consists of a neuroectoderm-derived bilayered cup, consisting of the inner neural retina, the outer retinal pigment epithelium (RPE), and a surface ectoderm-derived lens (1) (Fig. 1).

1.1.1 Retinal histogenesis

The adult mouse retina is made up of six distinct neurons (rod photoreceptors, cone photoreceptors, bipolar, amacrine, ganglion and horizontal cells), and one glial cell type, the Müller cells, which are arranged in three distinct layers or lamellae. The cell bodies of rod and cone photoreceptors are located in the outer nuclear layer (ONL); the cell bodies of amacrine, bipolar, horizontal cells and Müller cells are located in the inner nuclear layer (INL); and the cell bodies of ganglion cells and some displaced amacrine cells are located in the ganglion cell layer (GCL). The outer plexiform layer (OPL) and the inner plexiform layer (IPL) separate the cellular layers and are the locations of the neuronal synapses. The OPL contains synapses between photoreceptors, bipolar and horizontal cells and the IPL contains synapses between bipolar, ganglion and amacrine cells (2) (Fig. 2). Photoreceptor cells account for 70% of the cells in the adult mouse retina, and 97% of the photoreceptors are rods (3). RGCs, the projection neurons of the retina, make up only 2-3% of the total cells (3) and their axons lie on the surface of the retina and project through the optic nerve to visual

processing centers in the brain. In the INL, Bipolars make up 41% of all the cells in the layer, amacrines 39%, Müller glia 16%, and horizontal cells 3% (4).

The embryonic mouse neural retina consists of a layer of proliferating retinal progenitor cells (RPCs) that are dividing and will eventually give rise to all of the different retinal cell types. Lineage studies have shown that RPCs, like other CNS progenitors, are multipotent, such that a single progenitor cell can give rise to cell types as diverse as neurons and glia (5-8). The different retinal cell types are generated in a predictable sequence in two major waves of retinal histogenesis (9). The first wave peaks at E14.5, giving rise to early-born cell types, including retinal ganglion cells (RGCs), cone photoreceptors, amacrine cells, and horizontal cells. The second wave peaks at P4 giving rise to late-born cell types, including bipolar cells, and Müller glia. Rod photoreceptors are generated throughout the period of retinal histogenesis (9).

Figure 1. The development of a mouse retina

At E8.5, eyes first grow away from the ventral diencephalon and contact the surface ectoderm as an optic vesicle. The optic vesicle grows laterally and invaginates. At E10.5, the developing eye consists of a neuroectoderm-derived bilayered optic cup and a surface ectoderm-derived lens vesicle. The optic cup consists of inner neural retina and outer RPE (revised from Zhang SS. et al. Tissue culture studies of retinal development. *Methods* (2002) 28: 439-447)

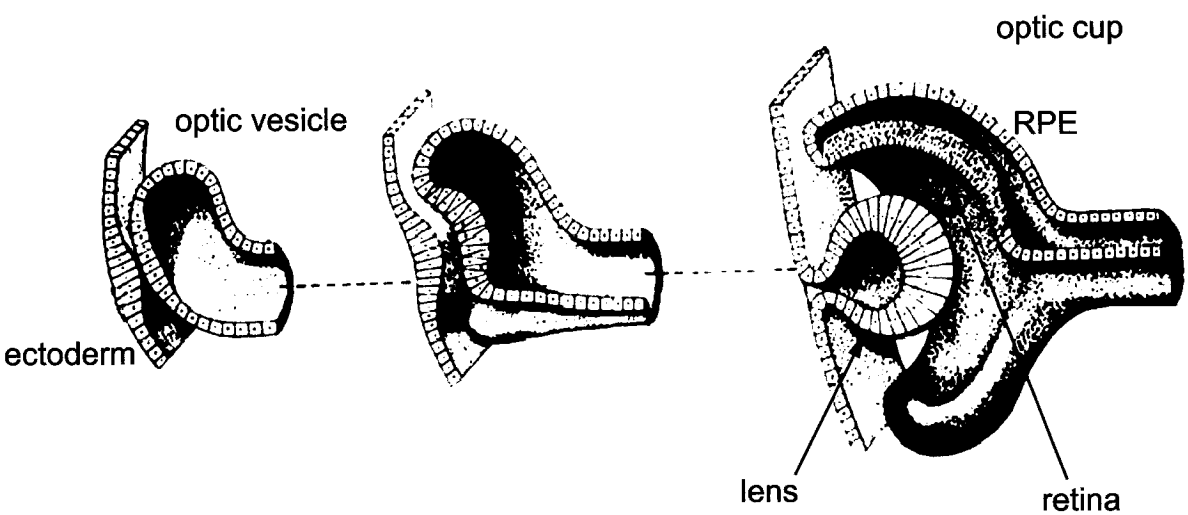

E8.5

E 10.5

Figure 2. The structure of the adult mouse retina

The adult mouse retina contains six neurons and one glial cell type, whose cell bodies are organized into the three different cell layers: outer nuclear layer (ONL), inner nuclear layer (INL) and ganglion cell layer (GCL). The cell bodies of rod and cone photoreceptors are located in the ONL; the cell bodies of amacrine, bipolar, horizontal and Müller glia cells are located in the INL; and the cell bodies of the ganglion cell layer and some displaced amacrine cells are located in the GCL. Dividing these nerve cell layers are two plexiform layers: outer plexiform layer (OPL) and inner plexiform layer (IPL), where synaptic contacts occur. Right panel is hematoxylin staining of a section from an adult mouse retina.

Abbreviations: R: rod photoreceptors; C: cone photoreceptors; M: Müller cells; B: bipolar cells; H: horizontal cells; A: amacrine cells; G: ganglion cells.

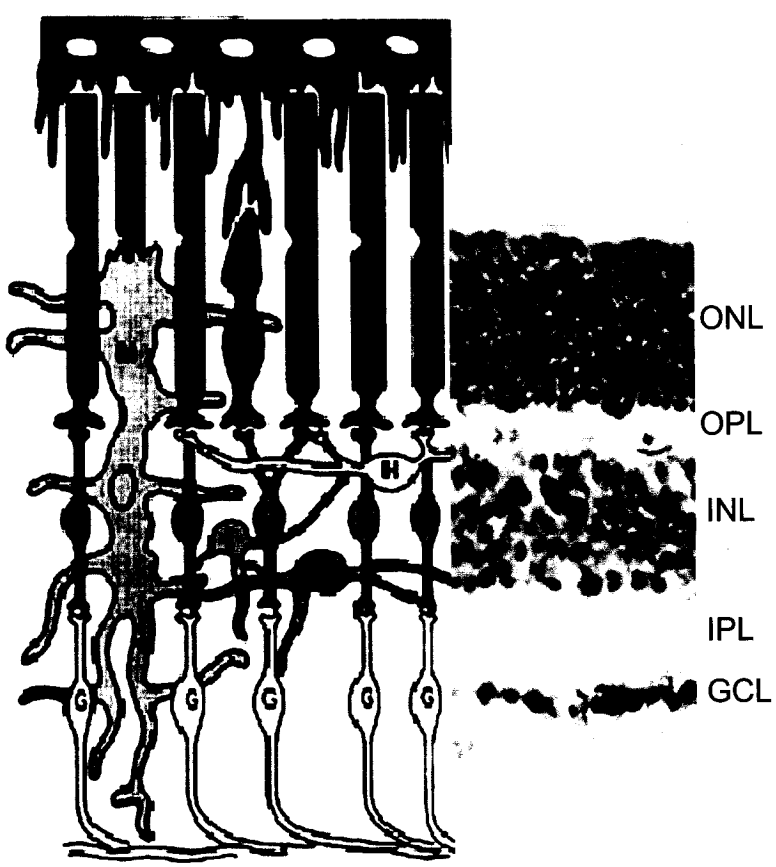
ONL
OPL
INL
IPL
GCL
H
G
G
G
G
G

Coordination of proliferation and differentiation of RPCs is of particular importance during retinal development. Because the interval in which the complete complement of retinal cells is produced overlaps with the interval in which RPCs exit the cell cycle and differentiate into mature retinal cells, RPCs have to balance two opposing forces: they must proliferate extensively and produce a sufficient number of cells, at an appropriate rate, for generating late cell types, but must also stop proliferating to produce the cell types that are born early. If there were not enough progenitor cells left at the end of histogenesis because they exited the cell cycle too early, then the late-born cell types would be diminished in the mature tissue (10). Conversely, if cells fail to exit the cell cycle at the appropriate time in development, there might be too many later-born cell types or a dysplasia could form, which, under certain circumstances, is the precursor to tumour formation (11).

The existing evidence indicates that proliferation and differentiation of RPCs are regulated by complex interactions between extrinsic cues and intrinsic factors. The intrinsic changes might be in part mediated by the cumulative effect of changing extrinsic signals to which RPCs were exposed during the course of retinogenesis (12).

1.1.2 Proliferation of RPCs during retinal histogenesis

Factors that regulate proliferation must ultimately exert their effects on the cell cycle, which is divided into four phases based on cellular activity. In S phase, the genome is replicated by DNA synthesis. In G2 phase, cells ensure that they have no DNA replication errors and prepare for mitosis. Mitotic cell division occurs in M phase. G1 phase is the primary interval for cell growth, but it is also the phase in which growth-promoting and -

inhibiting signals have a direct impact on whether a progenitor cell will exit from or continue progressing through the cell cycle. Proliferation-competent cells require mitogenic signals during early G1 to keep progressing through the cell cycle. Molecules such as fibroblast growth factor (FGF), epidermal growth factor (EGF), transforming growth factor (TGF), insulin-like growth factor (IGF), Hh and Wnt have been shown to act as mitogens for CNS progenitors (8, 13-15). Once a cell progresses past the restriction point (R) and into late G1, it is no longer dependent on mitogens and is intrinsically committed to progress through S phase (16).

Recent studies have shown that components of the cell-cycle machinery can have diverse and unexpected roles in the developing mouse retina. Rb proteins are thought to be central mediators of G1 phase progression, in that their phosphorylation state acts as a convergence point for proliferation signals. *pRb*-null mice die between E12 and E15, but chimeric mice containing *pRb*-null cells can be evaluated throughout development and show ectopic mitoses and increased cell death in the retina at E16.5 (17). These chimeric mice do not have retinal tumors, but chimeras with a double knockout of pRb and another Rb protein, p107, develop severe retinal dysplasia at E17.5 (18). However, the role of Rb in the retinal proliferation is still an enigma. Chen D et al. showed that *Rb/p107* loss does not affect progenitor proliferation in retinoblastoma, but perturbs cell cycle exit (19). D-cyclins are key regulators of G1 phase. Cyclin D1 is the predominant D-type cyclin expressed in RPCs and newborn *Cyclin D1*-null mice have hypocellular retinas due to reduced proliferation (20). But, proliferation still occurs in the *Cyclin D1*-null retina and this could be due to the persistent expression of Cyclin D3 or to a D-cyclin-independent mechanism. It appears that both may be responsible, since the combined inactivation of Cyclin D1 and Cyclin D3

further reduces RPC proliferation, but not completely (21).

In the retina, several homeobox genes that are expressed in RPCs may also serve as important regulators of proliferation by interacting with the cell cycle machinery. Over-expression of Optx 2, the *Xenopus* orthologue of Six 6, induces ectopic retinal tissue and expands the normal optic vesicle (22). Six 6 binds to the Kip 1 promoter in retinal cells and several co-repressors including Dach 2 are associated with this binding, indicating that Six 6 may be a direct repressor of Kip 1 transcription in RPCs. Consistently, Kip 1 mRNA and protein expressions are up-regulated in the *Six 6*-null retina (23). Chx 10 is among the most specific markers of vertebrate RPCs. It is expressed in all RPCs and a subset of bipolar cells (24) and may regulate cell cycle by regulating Kip1 activity through controlling Cyclin D1 levels (25).

The mitogens used by RPCs to regulate proliferation during retinal development are beginning to be identified. TGFα, bFGF and aFGF all promote RPC proliferation *in vitro* (8, 26, 27). Dissociated cells derived from the adult mouse RPE layer at the ciliary margin, when plated at clonal density, can form neural spheres if treated with FGF2 or EGF (28). Injection of insulin and FGF2 into toxin-treated chick eyes enhances the number as well as the differentiation of ganglion cells (29). Shh seems to be the relevant mitogen *in vivo* during mouse retina development since the conditional *Shh*-knockout mice have smaller eyes (30) and recombinant Shh-N stimulates the proliferation in the mouse developing retinal explant- and dissociated cell-cultures (31).

These studies raise some intriguing questions. Are cell cycle components direct targets of homeodomain transcription factors that have been implicated in proliferation

control? By what mechanisms do homeodomain transcription factors control RPC proliferation? For example, do they bind to and control transcription factors from *cis*-acting regulatory elements of cell cycle regulators or components of mitogen signalling components, or both?

1.1.3. Differentiation of RPCs during retinal histogenesis

Hetero-chronic cell mixing experiments have shown that RPCs display significant intrinsic changes in their potential to generate different cell types that change over time. For example, embryonic retinal cells, when cultured with an excess of postnatal retinal cells, do not adopt cell fates characteristic of postnatal RPCs (32-34), and vice versa (35). A current model of retinal development proposes that RPCs progress through a series of competence states during development, and each competence state favors specification of one or more cell fates. The competence states are presumably defined by cell-intrinsic properties that determine the responsiveness of the progenitor cell to extrinsic cues and the developmental potential of the progenitor (12).

Extrinsic signals can regulate retinal cell fate at two points. First, there are soluble factors produced by postmitotic neurons that provide feedback inhibition to progenitors to regulate cell-fate choices and which, at least for amacrine cells, seems to act on the progenitor before M phase (34). Secreted Shh molecules derived from differentiated RGCs act as negative feedback signals to modulate the further production of RGCs from the early retinal progenitor pool (36). Elevating Shh signal levels leads to a reduction of differentiated RGCs, whereas decreasing Shh signals suppresses RGC genesis during the peak period of

RGC production in the chick retina (36). Second, several factors have been shown to act on postmitotic cells to influence cell fate. Ciliary neurotrophic factors (CNTF) can inhibit rhodopsin expression and drive cells fated to be rods to express features of the bipolar neuron phenotype (37).

Notch signalling has been shown to be involved in the differentiation of both neurons and glia in the vertebrate retina (38). However, it is not clear whether changes in Notch signalling are instructive or simply permissive in regulating cell-fate choices in vertebrates. During the late stages of rat retinal development, introduction of Notch favours the development of Müller glia at the expense of neurons (39). This might be due to a block in the production of postmitotic cells from earlier, neuron-only competence states. Cells with high Notch signalling might pass into the last competence state, one in which they make Müller glia, without producing neurons *en route* to this state. Extensive production of Müller glia may then take place in the presence of Notch signalling, which might indicate a permissive rather than instructive role for Notch (12).

1.1.4 The development of mouse rod photoreceptor cells

The mouse retina contains two types of photoreceptors, cones and rods. Cones are responsible for daylight and color vision, while rods mediate dim light vision. Both cones and rods elaborate a specialized structure, the outer segment, in which visual pigments, rhodopsin in rods and opsin in cones, are concentrated.

Rod photoreceptors are generated throughout retinal development (32). The majority of rod precursors undergo terminal cell cycle exit after E19 and display remarkable regularity

in the onset of rhodopsin expression. These rod precursors do not express rhodopsin until approximately 5.5 to 6.5 days after their terminal mitosis (32). However, they display a characteristic pattern of heterochromatin in the nucleus, which is not seen in the other retinal cell types (7). Previous studies showed that postmitotic rods acquire this chromatin pattern before they express rhodopsin (40).

Before rhodopsin is expressed, there are two additional markers for the differentiating and differentiated photoreceptor cells: *Crx* and recoverin (Fig 3). *Crx* is a member of the otd/Otx homeobox gene family and is the earliest known marker of photoreceptor identity in the developing retina (39). During rodent development, *Crx* exhibits a biphasic expression pattern (39). First, *Crx* transcripts are found in developing cone photoreceptors at E12.5 in mouse and subsequently in developing rod photoreceptors. Second, *Crx* expression is up-regulated during the outer segment morphogenesis. *Crx* is expressed predominantly in postmitotic differentiating photoreceptor cells; its expression is also maintained in mature differentiated photoreceptor cells, as well as cone bipolar cells and a rare population of cells in the ganglion cell layer. Recoverin is an N-myristoylated 23 kDa calcium-binding protein from retina, which modulates the Ca^{2+}-sensitive deactivation of rhodopsin via Ca^{2+}-dependent inhibition of rhodopsin kinase, and it is expressed prior to rhodopsin expression (41).

There is accumulating evidence that rod development depends on short-range cell-cell interactions. In two studies of retinal development in rats, for example, it was found that rods develop in explant (42) and pellet (43) cultures, but not in dissociated cell cultures [42-43]. The signalling molecules that mediate these rod-promoting cell-cell interactions in culture remain to be determined, although at least some of them seem to be diffusible (44). Several

known molecules have been shown to act on the postmitotic rod precursors to accelerate rodent rod development in vitro, including retinoic acid (45), taurine (46), basic fibroblast growth factor (bFGF) (47) and S-laminin (48). Others have been found to inhibit such development, including transforming growth factor α (TGFα) (27), ciliary neurotrophic factor (CNTF) (49) and LIF (40).

Figure 3. A model of development of rod photoreceptor cells

Crx is expressed in postmitotic cells fated to give rise to photoreceptor cells soon after they exit the terminal mitosis. Rhodopsin is expressed in a fully differentiated rod and recoverin is expressed earlier than rhodopsin. Postmitotic rods exhibit a characteristic nuclear pattern of heterochromatin before they express rhodopsin.

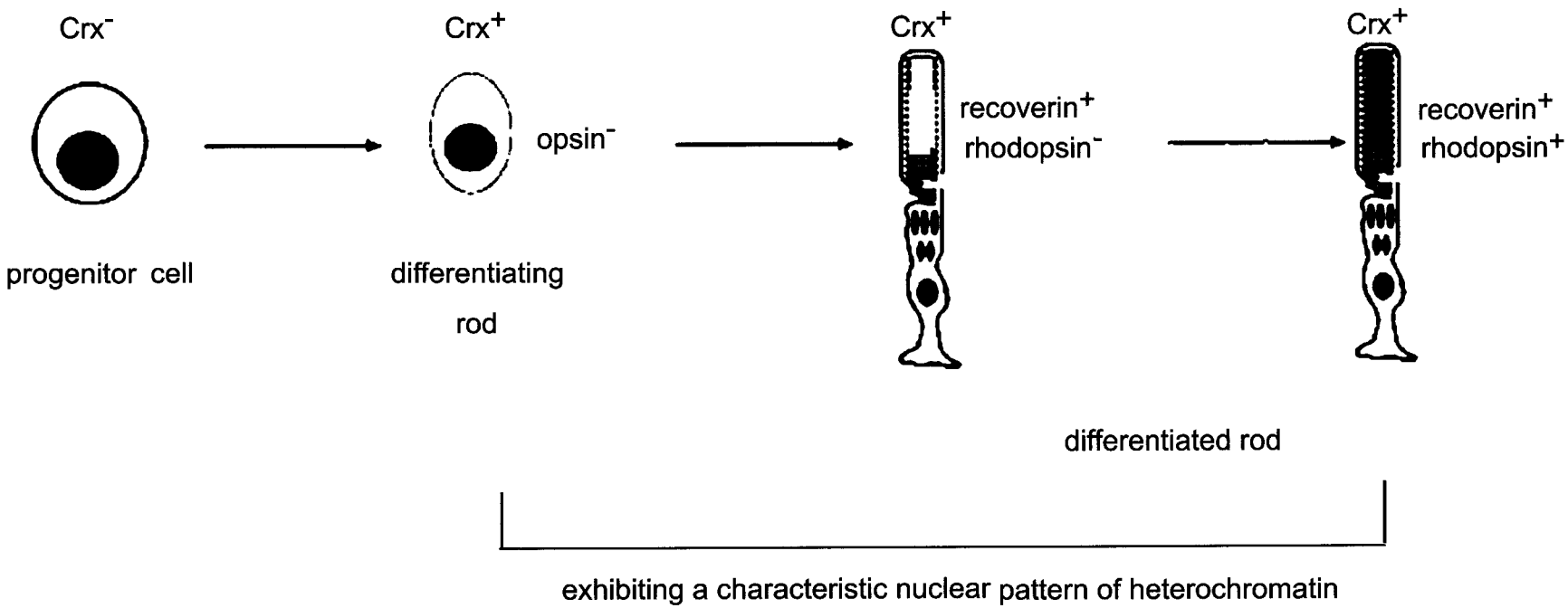
Crx-
Crx+
Crx+
Crx+
opsin-
recoverin+
rhodopsin-
recoverin+
rhodopsin+
progenitor cell
differentiating
rod
differentiated rod
exhibiting a characteristic nuclear pattern of heterochromatin

1.2 The Hedgehog signalling pathway

Hedgehog (Hh) was first identified by a genetic screen in the fruit fly *Drosophila* in 1980, which identified a number of mutations affecting embryonic and larval development. Hh mutant flies exhibit a continuous lawn of denticles projecting from the larval cuticle, suggesting the spines of a hedgehog, hence the origin of the name (50). Since then, several Hh homologs have been isolated from various vertebrate species. There are three hedgehog genes in mammmals: *Sonic hedgehog (Shh), Indian hedgehog (Ihh),* and *Desert hedgehog (Dhh).* The Hh genes encode a family of highly conserved secreted proteins that play a role in the development of a wide range of tissues (51, 52). Indian hedgehog is expressed in the gut and in cartilage and is important in postnatal bone growth (53). Dhh is expressed in the Sertoli cells of the testes, and mice homozygous for a null allele of *dhh* exhibit defective spermatogenesis (54). Sonic hedgehog is the most widely used of the three vertebrate homologues. Shh is responsible for patterning of the neural tube (55), the somites (56), the mouse tooth (57) and mediates the formation of the left-right axis in chicks (58).

1.2.1 Biogenesis of the Hedgehog proteins

In vertebrates, the Hh proteins are synthesized from ~45kD precursor proteins. Upon entry into the secretory pathway, the Hh precursor proteins undergo an internal autoproteolytic cleavage, which depends on conserved sequences in the C-terminal portion of the protein (59). This autocleavage generates a 19 kDa N-terminal peptide and a C-terminal peptide of 26-28 kDa (60). The N-terminal peptide is tightly associated with the surface of cells in which it is synthesized, while the C-terminal peptide is freely diffusible,

both *in vivo* and *in vitro*. It is a cholesterol nucleophile bound to the C-terminal end of the N-peptide that tethers Hh ligand to the cell surface (61). As a result of this tethering, a high local concentration of N-terminal Hedgehog peptide is generated on the surface of the Hedgehog-producing cells. N-terminal peptide is both necessary and sufficient for short- and long-range Hh signalling activities in *Drosophila* and vertebrates. In addition to cholesterol-coupling, analysis of Shh expressed in tissue culture cells has revealed a further lipid modification, palmitoylation of its most N-terminal cysteine, which is highly conserved in all Hh proteins (62). Palmitoylation of Hh proteins is distinctive in that it takes place within the secretory pathway, and it resolves into a stable amide linkage (63) (Fig. 4A). Although the mechanism of it is still poorly defined, some consequences have already implicated it not only for Hh protein generation and packaging but also in the distribution and reception of the Hh signal (63, 64).

1.2.2 Reception of the Hedgehog signals

After release from the Hh-producing cells, Hh signals act through the Patched (Ptc)-Smoothened (Smo) receptor complex located at the surface of Hh-receiving cells. The Hh signalling pathway activity is triggered by the stoichiometric binding of Hh ligand to its receptor Ptc (65), an apparent transmembrane transporter. In the absence of Hh, Ptc suppresses the activity of another receptor, the seven-transmembrane, G-protein coupled receptor (GPCR) Smo (66). The actual mechanism of suppression of Smo activity by Ptc remains unclear. The binding of Hh to Ptc, releasing its inhibition of Smo activity, culminates in the stabilization of the transcriptional factors: Cubitus interruptus (Ci) in *Drosophila,* and Gli TFs in vertebrates. In fact, Smo seems to be responsible for all of the

cellular responses to Hh since *Smo* null mutant mice are phenotypically identical with compound mutants for *Shh* and its close relative, *Ihh* (67).

The mechanisms by which Smo activation is regulated and coupled to downstream components remain enigmatic. In vertebrates, the situation is more complicated by the fact that there are three Ci-like Gli proteins Gli1, Gli2, Gli3, which mediate the activities of the Hh signal. In addition, at least two of them, Gli1 and Gli3, are themselves transcriptional targets of Hh signalling: Gli1 is activated (68) and Gli3 (69) is repressed in response to Hh signals. On Hh binding to Ptc, a macromolecular complex that is associated with microtubes, and includes Su(fu) (Suppressor of fused), Fu (Fused), protein kinase A (PKA), the Gli proteins and other possible components, acts to produce labile Gli activators. These are imported into the nucleus and transactivate target genes (Fig. 4B). The regulation of Gli activity takes place at many levels, including nuclear export and the presence of positive or negative cofactors (68-70).

Figure 4. Biogenesis and reception of Shh signaling pathway in vertebrates

A. Biogenesis of Shh signaling pathway in vertebrates.

The Shh precursor is processed to generate the N-SHH morphogen, to which two modifications are introduced: a cholesterol group at the C-terminal and a palmitoyl moiety at the N-terminal. Cholesterol is added by C-SHH, whereas palmitoyl is added by an unknown component in vertebrates.

B. Reception of Shh signaling pathway in vertebrates.

There are combined receptors of Shh signal, Ptc and Smo, located at the surface of Shh receiving cells. On Hh binding to Ptc, the inhibition of Smo by Ptc is released. Thus, a macromolecular complex that is associated with the cytoskeleton, and includes Su(fu) (Suppressor of fused), Fu (Fused), protein kinase A (PKA), the Gli proteins and other possible components, acts to produce labile Gli activators. Zinc-finger transcription factors of the Ci/Gli (Gli 1–3) family, which might be associated with the intracellular complex and translocated to the nucleus by activation of the pathway, act at the last step of Shh signaling. The regulation of Gli activity takes place at many levels, including nuclear export and the presence of positive or negative cofactors.

(pictures taken from Marti E. et al. Sonic hedgehog in CNS development: one signal, multiple outputs. *Trends in neurosciences.* 2002 (2): 89-96)

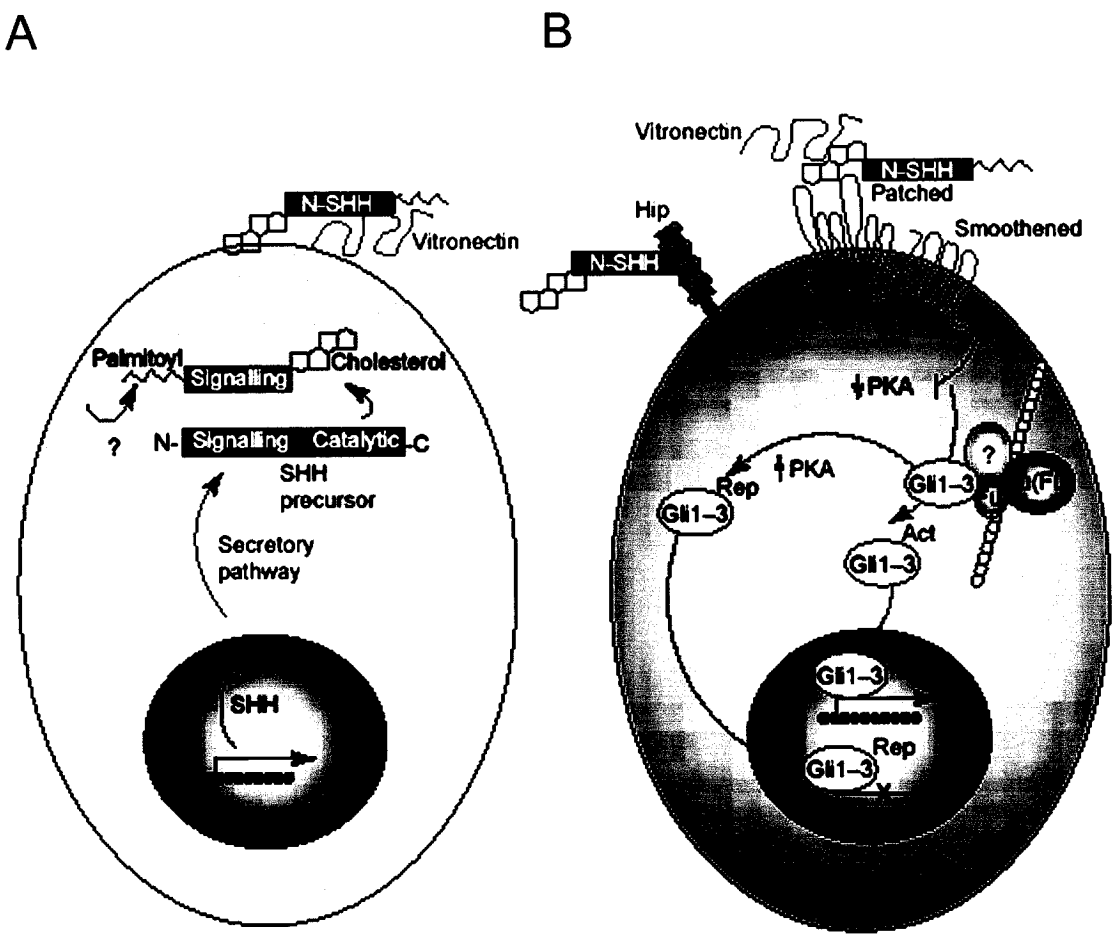

Shh sending cells

Shh receiving cell

1.2.3 Functions of the Hedgehog signalling pathway

Since their isolation in the 1990s, members of the Hh protein family have come to be recognized as key mediators of many fundamental processes during the growth, patterning, and morphogenesis of many different organs in the body plans (reviewed in (71)). Although the precise cellular roles of Hh signals are still under scrutiny, it is clear that they can elicit different responses depending on the context in which the signals operate. Thus, Hh signals have been shown to regulate cell fate specification, cell proliferation, and cell survival in different target cells (72, 73). Signalling can be short- and long-range, direct and indirect (through the activation of a signalling relay) (74, 75), and importantly, concentration-dependent, evoking distinct molecular responses at discrete concentration thresholds (a classic morphogen activity) (76).

1.2.3.1 Contributions of Shh to retinogenesis

Shh signals play an important role during vertebrate retinogenesis. *Shh* is expressed in the retinal ganglion cell (RGC) layer from E12 to adult, whereas *Ihh* and *Dhh* expression is not detected in the neural retina at any stage (77). However, Ihh is expressed in the embryonic extraocular mesenchyme (78) and likely plays a role in scleral development (77, 79). The developing neuroblasts respond to the Hh signal by expressing the Hh target genes *Ptc1* and *Gli1* (31). In the conditional *Shh* knockout mice, *Gli1* expression is downregulated, indicating that Shh derived from RGCs is required for the maintenance of Hh target gene expression in the retina (30).

There is some evidence to show the effects of Shh on the proliferation of developing retina. Recombinant Shh-N stimulates RPC proliferation in mouse retinal explant- and

dissociated cell-cultures, while anti-Hh antibody blocks the proliferation under the same conditions (31). Conditional disruption of the *Shh* gene in RGCs results in a smaller eye (30).

Shh is required for retinal organization. The conditional *Shh* knockout mice show lamination defects, as indicated by the disorganized photoreceptor cell layer, whereas recombinant Shh-N treated mouse retinal explants maintain the normal organization (30). In *Shh* mutant zebrafish (*sonic yu (syu)* mutants), the lamination of retina is also disrupted (80).

Shh also plays an important role in the differentiation of RPCs. Secreted Shh molecules derived from differentiated RGCs act as negative feedback signals to modulate the further production of RGCs from the early retinal progenitor pool (36). In addition, recombinant Shh-N protein stimulated the differentiation of Müller glia, amacrine and bipolar cells at the expense of rod photoreceptors, while anti-Hh antibody (5E1) had the opposite effect (except for the rod photoreceptors, which was no significant difference with control) to the retinal explants (YP Wang and V Wallace, unpublished data).

1.2.4 Constitutive activation of the Hedgehog signalling pathway

There were two activating somatic missense mutations in the *Smo* gene that were identified in sporadic human basal cell carcinoma (BCC) (81). These mutations render the Smo protein insensitive to regulation by Ptc. One of the mutations is a missense mutation at base pair 1,685, designated M1, which is predicted to change Arg 562 (CGG) to Gln (CAG) in the carboxy-terminal cytoplasmic tail of Smo (81). This basic residue is conserved in *Drosophila*, rat and mouse. Another mutation is a G-to-T transversion at base pair 1,604 (M2), changing codon 535 from Trp to Leu in the seventh transmembrane domain of human Smo (81) (Fig. 5). The Trp residue at codon 535 is conserved among all described Smo

protein sequences. It is not clear how these mutations generate a form of Smo that is insensitive to antagonism by Ptc. Ectopic expression of Smo-M2 in the neural tube is shown to drive constitutive activation of Hh signalling pathway and mimic multiple concentration-dependent actions of Shh, including activation of ventral marker genes, suppression of dorsal markers and induction of several Shh-dependent neural cell types, while the wild-type Smo transgenic mice do not have similar phenotypes (82).

Figure 5. Two activating mutations of Smo

There are two activating mutations of Smo from the study of three sporadic human basal cell carcinoma (BCC) tumors. M1 is located at base pair 1,685 from C-terminal cytoplasmic tail of Smo, changing 562 Arg to Gln. M2 (Smo^c) is identified at base pair 1,604 in the seventh transmembrane domain of Smo, changing 535 Trp to Leu. The mechanisms by which Ptc inhibits the activity of Smo at the absence of Hh ligand and by which mutant Smo escapes such an inhibition remain unknown.

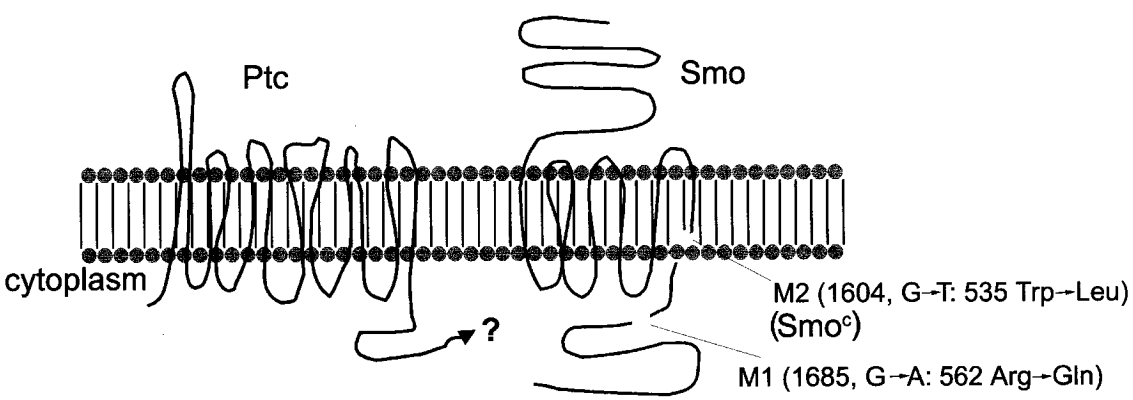
Ptc
Smo
cytoplasm
?
M2 (1604, G→T: 535 Trp→Leu)
(Smo^c)
M1 (1685, G→A: 562 Arg→Gln)

1.3 Retroviral delivery as an approach to modulate gene expression in the retina

The neural retina can be isolated from mouse embryos and maintained in culture for more than one week (30). Several aspects of explant cultures mimic *in vivo* development, including neuronal differentiation and lamination (42). Retroviral vectors are widely used as a tool to express transgenes in retinal cells because of their high gene-transfer efficiency and easy manipulation (83).

1.3.1 The life cycle of retroviruses

Retroviruses are naturally occurring, RNA-containing viruses. The single-stranded RNA genome is encapsulated in an icosahedral protein shell and lipoprotein envelope. Retroviruses enter the host cell through an interaction at the cell surface, presumably via a specific protein receptor. Viral envelope proteins, encoded by *env* genes, bind to the host receptor and mediate entry. Once in the cytoplasm, the viral RNA is reverse-transcribed into DNA by the viral enzyme reverse transcriptase, a product of the viral *pol* gene that is present in the viral particle (84). The viral DNA then integrates into the host genome where it is referred to as a provirus. Integration of the genome of most retroviruses requires that the cells go through an S phase (85), and thus only mitotic cells will serve successfully as hosts for integration of most retroviruses. Once integrated, a wild-type replication-competent provirus proceeds to make more retroviruses by expressing the viral structural genes, *gag* (encoding packaging proteins), *pol, env.* After assembly of the virus, a complete, infectious particle buds from the host plasma membrane.

An infectious virus stock is made from cloned vectors encoded by bacterial plasmids into cell lines called packaging lines. Once in a cell line, transcription proceeds from the viral promoter encoded by the plasmid, generating an RNA viral genome. The viral genome is then encapsulated by viral structural proteins and infectious viral particles are produced by budding from the surface of cells. The supernatant produced by such cells comprises a virus stock. The titered stock is then used to infect cells *in vivo* or *in vitro*.

1.3.2 Replication-incompetent retrovirus

A retroviral vector is a retrovirus that has been modified to include heterologous genes for the purposes of transduction and expression. Replication-competent retroviral vectors encode all of the *cis*-acting viral sequences necessary for the viral life cycle. Deletion of some or all of the genes encoding virion structural proteins was carried out to create room for inserted genes and to cripple the virus, making it replication incompetent.

The most useful retroviral vector is the replication-incompetent retroviral vector that can not spread, ensuring that cells are marked through lineage and not from horizontal spread. The *gag, pol* and *env* structural genes are deleted, while the ψ packaging sequence is preserved, which is necessary for recognition of the viral RNA for encapsidation into the virus particle (86). The preserved sequences also include reverse transcription signals, integration signals, and viral promoter, enhancer, and polyadenylation sequences. Using the transcription regulatory sequences provided by the virus, cDNA could be expressed in the vector. Since the viral transcript does not encode any of the structural proteins required to make a viral particle, these are supplied by the packaging cell lines, which have been stably transfected to express the *gag, pol* and *env* genes (87). These viral genes do not contain the

cis-acting packaging sequence, ψ, and thus do not become encapsidated. Therefore, the packaging cell lines make infectious viral particles that do not contain the genes *gag, pol* and *env*; once integrated to the host cells, no new virions are produced and the viral genome can only pass to progeny through cell division.

The most commonly used packaging cell lines for the replication-incompetent retrovirus vectors are Phoenix cells. Phoenix is a second-generation retrovirus producer line based on the 293T cell line, which is used for the generation of helper-free ecotropic and amphotropic retroviruses (88). The unique feature of this cell line is that it is highly transfectable with either calcium phosphate or lipid-based transfection protocols-- up to 50% or higher of cells can be transiently transfected. According to the category of the *env* glycoproteins that interact with different host cell receptors, there are two classes of Phoenix packaging cell lines, Phoenix-Amphotropic (Amp) and Phoenix-Ecotropic (Eco). The ecotropic *env* glycoprotein allows entry only into rat and mouse cells via the ecotropic receptor on these species. It does not allow infection to humans and, thus, is considered relatively safe for gene transfer experiments. The amphotropic *env* protein allows entry into a wider range of mammalian species, including human.

1.4 Objective

Lineage analyses have indicated that mitotic progenitor cells in the mouse retina are multipotent throughout development (89). In terms of their competence to produce distinct types of cells at different stages of development, these progenitors are intrinsically different, so that they go through a series of changes in intrinsic properties that control their

competence to make different cell types and extrinsic cues that influence the ratios of the cell types that they produce (9).

It is now well established that this process of cell-fate determination is regulated by a combination of extrinsic and intrinsic influences (12). However, how these two influences combine to contribute to that is still unclear. Shh is an extrinsic factor that plays a role in retinal histogenesis. Although RPCs appear to be targets of Hh signalling in the retina, it is not clear if all of the effects of Hh signalling are mediated cell autonomously, i.e. directly on RPCs, or non-cell autonomously, i.e. via the production of secondary signalling molecules. The **objective** of my project was to characterize the consequences of cell autonomous activation of the Hh signalling pathway in RPCs. Constitutive activation of Hh signalling in cells was achieved by driving the expression of a mutant form of Smoothened (M2, Smo^c). This approach allowed us to distinguish between direct and indirect effects of Hh signalling on precursor cells. Smo^c expression was induced in retinal precursor cells by retroviral infection in retinal explant cultures and infected cells were identified by the expression of the eGFP reporter gene that was encoded in the virus. I have compared clone size, proliferation, and cell diversification between Smo^c- and eGFP-retrovirus infected cells.

A journey of a thousand miles must begin with a single step.
- Lao-tzu

Materials and methods

2.1 Retrovirus vectors

The vector pCLE-Smo^c (containing the activating mutation M2 in the *Smo* gene) was obtained from Dr. Gord Fishell. The retroviral vector pMXIE, which contains the reporter gene eGFP downstream of an IRES, was obtained from Dr. Rod Bremner. The Smo^c-retrovirus was generated by subcloning a 2.5 kb fragment of Smo^c into an EcoRI site between the LTR and IRES-eGFP sequence of the pMXIE retroviral backbone, using standard cloning methods (90). The reselecting construct was mapped to confirm the orientation of the Smo^c fragment.

To confirm the orientation of the Smo^c fragment, one restriction enzyme, BamHI was chosen, according to the restriction map.

2.2 Production, concentration and titration of retroviruses

To produce the retrovirus, plasmid DNA corresponding to Smo^c- or eGFP-pMXIE constructs were transfected into the Phoenix-Eco packaging cell line by calcium phosphate precipitation, according to the protocol from the Nolan lab (http://www.stanford.edu/group/nolan/protocols/pro_helper_free.html).

48 hours after transfection, the viral supernatant was filtered through a 0.45 μm filter, poured into an ultra clear centrifuge tube and spun in a JA25.50 rotor at 21,000 rpm for 2 to 2.5 hours in the Beckman® AVANTI™ J-25I centrifuge, at 4 °C. The supernatant was then discarded and the pelleted virus was resuspended in approximately 200 μl of fresh retinal explant culture medium, containing 4 μg/ml polybrene. The pelleted virus was dissolved by pipetting (50-100 times) and the resulting stock was stored in 10 μl aliquots at -80 °C.

To determine the virus titer, NIH 3T3 cells were plated in a 24-well dish at 30,000 cells per well (500 μl medium for the first well, 450 μl medium per well for the other wells) on day 1. The following day, 1 μl concentrated retrovirus was added in the first well and mixed. A serial 10-fold dilution panel of virus was then established across the culture plate. 48 hours after infection, the NIH 3T3 cells were stained with anti-GFP antibody and the number of gfp^+ cells was determined to calculate the retrovirus titer. The infection efficiency of retrovirus was calculated with colony-forming units per ml (CFU/ml), according to the following formula:

Titer (CFU/ml) = number of gfp^+ cells / volume of retrovirus (ml)

2.3 Activation of the Hh signalling pathway driven by Smo^c-retrovirus in C3H 10T 1/2 cell line

The C3H 10T ½ cell line was established from mouse embryonic fibroblast cells. These cells undergo osteoblast differentiation in response to Hh as measured by *Gli1* expression in Hh-stimulated cells (91), so it provides a useful model to test the activation of the Hh signalling pathway by inspecting *Gli 1* expression.

To test the activation of the Hh signalling pathway driven by Smo^c expression, we infected the C3H 10T ½ cells with Smo^c- or eGFP-retroviruses. At noon of day 1, 8 x 10^5 C3H 10 T ½ cells were plated in each 60mm petri dish. As a positive control, 2 μg/ml recombinant Shh-N protein (a gift from Dr. Baker, Biogen) was added in one petri dish at the time the cells were plated. The following morning, Smo^c- or eGFP-retroviruses at the concentration of 10^6 CFU/dish were added in the other petri dishes individually. All of the cells were harvested two days following retrovirus-infection. Expressions of *Hprt* and the

downstream target gene of the Hh signalling pathway, *Gli1*, were examined by RT-PCR analysis (Appendix A).

2.4 Cell and retina explant culture

NIH 3T3, C3H 10T ½ and Phoenix-Eco cells were cultured in DMEM (Gibco, #10569-010), containing 10% heat-inactivated fetal calf serum (FCS) (Sigma, F-1051), 100 U/ml penicillin/streptomycin (Gibco, #15070-063), at 37°C, in 5% CO_2.

All retinal tissues were obtained from C57/BL-6 mice. To time the pregnancies, female mice were caged with males overnight and removed the next morning; the presence of a vaginal plug was considered day 0 of the pregnancy. Retinas from E18.5 mice were dissected free of RPE and lens, flattened onto a filter (Whatman, 0.8μM, #4198002) which was then put in 500 μl of culture medium (50% DMEM, 50% HAMS F-12, 1% Sato's ($T3^-$, $T4^-$), 10 μg/ml Insulin, 60 μg/ml NAC, 10 μg/ml Gentamycin) and cultured at 37°C, in 8% CO_2 (30). Sato's ($T3^-$, $T4^-$) contains 100 mg/ml Apotransferin (Sigma, T-1147), 10 mg/ml BSA (Sigma, A-4161), 6 μg/ml Progesterone (thaw in 100% ethanol first, Sigma, P-8783), 1.6 mg/ml Putriscine (Sigma, P-7505) and 4 μg/ml Sodium Selenate (Sigma, C-5261). For the retina explants cultured with the addition of 10% heat-inactivated FCS, the medium contained 45% DMEM, 45% HAMS F-12, 10% heat-inactivated FCS, 1% Sato's, 10 μg/ml Insulin, 60 μg/ml NAC, 10 μg/ml Gentamycin. The medium was refreshed every three days by replacing half of the culture medium with fresh medium.

To infect retinal explants with retrovirus in bulk analyses of infected cells, the first 6 μl of the concentrated retrovirus was dropped to cover the retinal explant on the filter one to two hours after it was put in the medium. In order to increase the infection efficiency,

another hour later, the second 6 μl of the concentrated retrovirus was dropped on top of the retinal explant. The titer of the concentrated eGFP-retrovirus was always several-times greater than that for the Smo^c-retrovirus, however, the infection efficiency of the eGFP-retrovirus was considerably lower than that of the Smo^c-retrovirus when comparable titers of retroviruses were used to infect retinal explants. Therefore, for bulk analyses of infected cells, 3 times greater titer of the eGFP-retrovirus was used to infect retinal explants. Considering that the half-life of retrovirus is only 3-6 hours at 37°C (92) and the volume of retrovirus covering retinal explant was so small, I did not wash the retrovirus-infected retina explants after infection.

To infect retina explants with retroviruses in clonal analyses, retina explants were only infected once with Smo^c- or eGFP-retroviruses at same titer, 10^6 CFU/ml.

2.5 Dissociation of retina explants

To dissociate retinal explants into single cell suspensions, one explant was placed in 250 μl Ca^{2++}, Mg^{2++}-free Dulbecco's Phosphate Buffered Saline (PBS), with 0.1 mg/ml trypsin, and incubated in a 37 °C water bath for 50 minutes. The digestion was stopped by adding 250 μl of 20% heat-inactivated FCS/MEM/DNase I (0.2 mg/ml) and the tissue was triturated 8 times to generate a single cell suspension. An aliquot of cells was removed for counting and the number of cells in the suspension was counted and then spun at 1000 rpm for 5 minutes. The cell pellet was resuspended in MEM containing 0.01 mg/ml insulin and the cell suspension was adjusted to a final concentration of 10^7 cells/ml. 15 μl of the cell suspension was pipetted onto Poly-D-lysine coated glass slides (VWR Canlab, #48323-185), and the slides were incubated at 37 °C in a water bath for 45 minutes to allow the cells to

adhere. The liquid on the slide was removed with filter paper, and the cells were fixed with 4% paraformaldehyde (PFA) for 10 minutes and processed for further immunohistochemistry staining or air-dried and stored at -20 °C.

2.6 Tissue embedding and sectioning

To process explanted tissue for cytosections, the retina explants were first fixed in 4% PFA at 4 °C for 2 hours, rinsed 3 times with 1xPBS (with calcium chloride and magnesium chloride, Sigma, #D8662) and cryoprotected in 30% sucrose/0.1M phosphate buffer overnight at 4 °C. The following day, the equilibrated retina was embedded in a 50:50 mixture of 30% sucrose:OCT (Tissue Tek 4583), frozen in liquid nitrogen and stored at -80 °C. The embedded tissues were cut at 8 μm for immunohistochemistry staining and 12 μm for *in situ* hybridization using a Leica CM 1850 cryostat. The sections were air-dried before further experiments or stored at -20 °C.

2.7 Immunohistochemistry and nuclear labeling

The sections or dissociated cells were permeabilized with 70% ethanol, washed 3 times with PBS, and incubated in the primary antibody diluted in 10% goat serum in PBS for two hours at room temperature. The antibodies used in this study are listed in Table 1 (Appendix B) (93-98). The fluorescent conjugated secondary antibodies (Table 2) (Appendix C), diluted in 2% goat serum in PBS, were incubated for 1 hour at room temperature. To visualize the nuclear morphology, cells were counterstained with the fluorescent DNA-

binding dye bisbenzimide (Hoechst) for 5 minutes and mounted with fluorescent mounting medium. Staining was visualized on a Zeiss fluorescent upright microscope.

2.8 BrdU incorporation and staining

To label cells in S-phase, E18.5 mouse retinal explants that had been cultured for 3 days were incubated with 20 μM BrdU for the last 20 hours of culture period. For double immunohistochemistry staining with anti-GFP and anti-BrdU antibodies, cells were stained first with anti-GFP antibody, post-fixed in 70% ethanol for 10 minutes, treated with 2N HCl for 20 minutes to denature the nuclear DNA, and neutralized with 0.1 M Tris (pH8.8)/0.1% Tween-20 for 5 minutes. Cells were then incubated in anti-BrdU antibody, following the standard immunohistochemistry staining protocol.

2.9 TUNEL staining

The air-dried sections of the retrovirus-infected explants were rinsed with 1x PBS for 10 to 30 minutes, permeabilized with a freshly made solution of 0.1% sodium citrate and 0.1% Triton X-100 for 3 minutes and washed twice with 1x PBS. TUNEL reaction mixture (*in situ* cell death detection kit, from Roche, #1684795) 100 μl was added on every slide and the slides were incubated at 37 °C in the dark with coverslips for 60 minutes. The slides were washed twice with 1x PBS and mounted with fluorescent mounting medium.

2.10 *In situ* hybridization and staining

The sections of the retrovirus-infected explants were cut at 12 μm to superfrost slides (Fisherbrand®, #12-550-15) and air-dried for at least 2 hours. The *CRX* probe were thawed quickly, diluted (1:1000) in hybridization solution (Appendix D), vortexed and denatured at 70 °C for 10 minutes. 100 μl of the denatured probe was pipetted onto each slide and covered with a coverslip (22mm x 50mm). The slides were placed in a box containing 2 sheets of 3mm whatmann paper, which was pre-soaked with a 1:1 mixture of 50% Formamide: 1x salt (Appendix D) and incubated at 65 °C overnight.

The following morning, the slides were transferred to a slide box with a removable glass rack and washed with wash buffer (1x SSC, 50% formamide, and 0.1% Tween-20) 3 times at 65 °C, 15 minutes for the first wash, 30 minutes for the second and third washes. The slides were then washed in 1x MABT (0.1M maleric acid, 0.15M NaCl, 0.1% Tween-20, ph=7.5) twice for 30 minutes at room temperature.

The slides were incubated in blocking solution (10% sheep serum, 2% blocking reagent (Gibco, #1096176), 1X MABT) at RT for at least 1 hour in the humidified box. After blocking, the anti-DIG antibody (BM, #1093274) was diluted 1:2000 in blocking solution and added to the sections. These sections were incubated in a humidified box at 4 °C overnight.

The following morning, slides were washed 4 to 5 times with 1x MABT for 20 minutes, each time with rocking. Slides were then equilibrated twice in staining buffer (Appendix E) for 10 minutes each, with rocking at RT. The slides were transferred to staining buffer containing 4.5 μl /ml NBT (4-Nitro blue tetrazolium chloride, Roche, #1383213) and 3.5 μl/ml BCIP (5-Bromo-4-chloro-3-indolyl-phosphate, Roche, #1383221)

and incubated at RT in the dark overnight. The next morning, slides were washed several times with 1x PBS, mounted with a 1:1 mixture of glycerol:PBS and sealed with clear nail polish, stored at 4 °C.

2.11 Statistical analysis

When scoring, all of the data were from three retinal explants per condition. For scoring rod photoreceptors, approximately 500 cells were counted from each retina, whereas for other cell types, approximately 1000 cells were counted from each retina. For scoring the locations of retrovirus-infected cells, approximately 500 cells were counted from each retina. For clonal analysis, approximately 300 clones were counted from each retina.

All data are presented as mean ± SD (standard deviation). Difference between Smo^c- and eGFP-retroviruses was evaluated for statistical significance using two-tailed, unpaired Student's *t*-test. * indicates $p < 0.05$, ** indicates $p < 0.005$.

A theory must be tempered with reality.

- Jawaharlal Nehru

Results

3.1 Generation and titration of the retroviruses

To construct the Smo^c retroviral vector, the 2.5 kb fragment corresponding to Smo^c was subcloned into the EcoRI site of pMXIE plasmid. To confirm the orientation of the Smo^c fragment (Fig. 6A), the subcloned plasmid was digested with BamHI. The Smo^c fragment was inserted in the correct direction (Fig. 6B), as BamHI digest liberated a 5.9 kb and a 2.5 kb fragments (Fig. 6C). The Smo^c- and eGFP-retroviral vectors were transfected into the Phoenix-Eco packaging cell line and 48 hours later, supernatants were collected and concentrated (see materials and methods 2.2).

To determine the retrovirus titer, the centrifuge-concentrated virus stocks were titrated on NIH 3T3 cells in a 10-fold dilution series. The viral titer was determined by counting the total number of gfp^+ cells in each well divided by the volume of virus used in the well. The concentrated Smo^c-retrovirus titer ranged from 10^7 to 10^8 colony-forming units (CFU) per ml and the concentrated eGFP-retrovirus titer ranged from 10^8 to 10^9 CFU per ml.

Retinal explants from E18.5 mice were infected twice in the interval of one hour, each time with 6 µl concentrated Smo^c- or eGFP-retroviruses. Three times greater titer of eGFP-retrovirus was used to infect retinal explants. After 7 days, retinal explants were dissociated into single cell suspensions, stained with anti-GFP antibody and the proportion of gfp^+ cells was quantified. The data shown below was just an illustration of the percentage of infected cells at 7 days, rather than an indication that Smo^c-expression promoted RPC proliferation.

virus	experiment 1	experiment 2	experiment 3
eGFP	1.1% ± 0.1%	4.4% ± 0.5%	1.6% ± 0.4%
Smo^c	2.4% ± 0.6%	5.0% ± 0.5%	5.2% ± 2.2%

Table 3. Percentage of gfp^+ cells in E18.5 retinal explants 7 days post-infection.

3.2 Smo^c expression activates the Hh signalling pathway in C3H 10T½ cells, an Hh-responsive osteoblast cell line

To test whether the expression of Smo^c results in activation of the Hh signalling pathway, we infected an Hh-responsive osteoblast cell line, C3H 10T1/2, with Smo^c- or eGFP-retroviruses. The infected cells were cultured for 2 days, and RNA was extracted with Trizol reagent. First strand cDNA was synthesized and gene expression was analyzed by PCR. As controls, RNA was also isolated from C3H 10T1/2 cells that were treated with or without recombinant N-terminal fragment of Shh (Shh-N). *Gli 1* expression was increased in Smo^c-infected and Shh-N-treated cells, but not in eGFP-infected or non-treated cells. Thus Smo^c expression induced activation of Hh target gene expression (Fig. 7).

3.3 Cell-autonomous activation of the Hh signalling pathway stimulates the proliferation of retinal precursor cells

To determine whether the constitutive activation of the Hh signalling pathway promoted RPC proliferation, we compared proliferation of retrovirus-infected cells in retinal explants. E18.5 mouse retinal explants were infected with Smo^{c}- or eGFP-retroviruses and cultured in serum-free medium for 3 days (explants were cultured in defined serum-free medium to avoid any effects of serum on proliferation). To label cells in S-phase, the retinal explants were pulsed with Brdu in the last 20 hours of the culture. The retinal explants were dissociated and double stained with anti-GFP and anti-BrdU antibodies. There was a two-fold increase in the proportion of S-phase cells amongst the Smo^{c}-infected cohort compared with the eGFP-infected cohort (Fig. 8A). There was no change in the percentage of S-phase cells amongst the uninfected cohort, indicating that the effects of the Hh signalling pathway on RPC proliferation were cell-autonomous (Fig. 8B).

Figure 6. Retroviral vectors

A. Schematic of the pMXIE retroviral vectors.
Smo^c (M2) cDNA was inserted into pMXIE retroviral vector between LTR and IRES-eGFP sequences.

B. Simplified restriction map of the Smo^c-pMXIE plasmid.
The pMXIE plasmid backbone is 5.8 kb. The Smo^c fragment is appromixately 2.5 kb and was inserted into the EcoRI site of the pMXIE plasmid.

C. Restriction enzyme, BamHI, digestion of retroviral plasmids
The backbone of the BamHI-digested plasmid pMXIE contained a 5.9 kb single fragment, while the BamHI-digested Smo^c-pMXIE plasmid contained two fragments: 5.9 kb and 2.5 kb fragments.

A

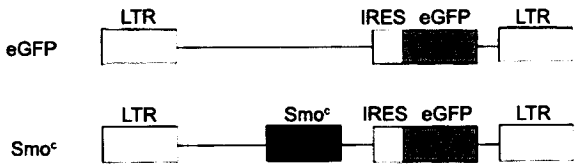
LTR
IRES eGFP
LTR
eGFP
LTR
Smoc
IRES eGFP
LTR
Smoc

B

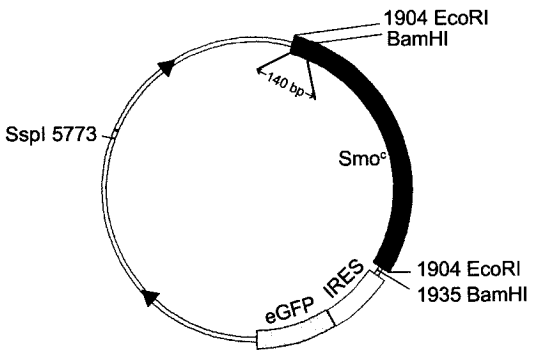
1904 EcoRI
BamHI
140 bp
SspI 5773
Smoc
1904 EcoRI
1935 BamHI
eGFP
IRES

C


λ DNA / Hind III
Smoc-pMXIE / BamHI
pMXIE / BamHI
6557 bp
4881 bp
2322 bp

Figure 7. RT-PCR analysis of gene expression in C3H 10T 1/2 cells

C3H 10T 1/2 cells were treated with or without recombinant Shh-N (2 μg/ml), or infected with Smo^{c}- or eGFP-retroviruses, cultured for 2 days and subjected to RT-PCR analysis for *Gli1* and *Hprt* expression. The E18.5 retina lane refers to RNA from acutely dissected E18.5 mouse retinas in which the Hh signaling pathway is activated, as evidenced by *Gli1* expression in this sample. Water control, without template, was used as a negative control for the PCR reaction.

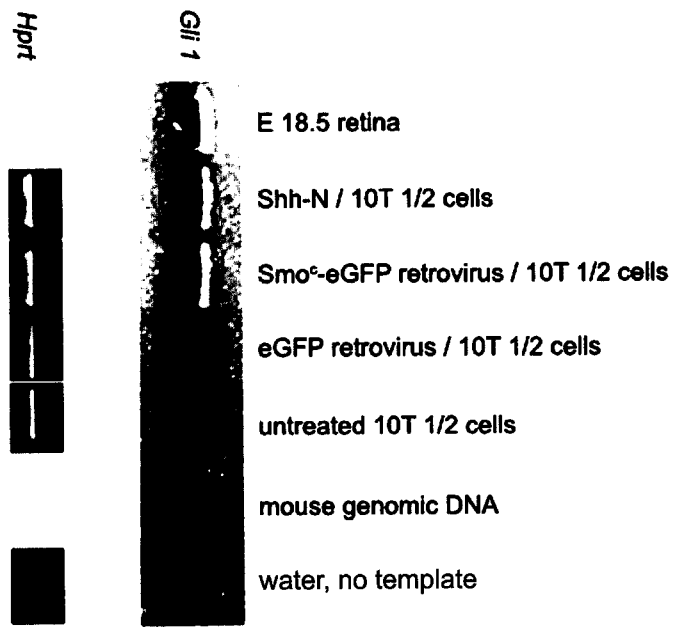
Hprt
Gli 1
E 18.5 retina
Shh-N / 10T 1/2 cells
Smo^c-eGFP retrovirus / 10T 1/2 cells
eGFP retrovirus / 10T 1/2 cells
untreated 10T 1/2 cells
mouse genomic DNA
water, no template

Figure 8. Cell-autonomous activation of the Hh signaling pathway promotes RPC proliferation.

E18.5 mouse retinal explants were infected with Smo^{c}- or eGFP-retroviruses, cultured for 3 days, and pulsed with BrdU for the last 20 hours of culture. At 3 days, retinal explants were dissociated into single cells and stained with anti-GFP and anti-Brdu antibodies.

A. Proportion of $BrdU^{+}$ cells amongst the retrovirus-infected cells (gfp^{+} cohort).

B. Proportion of $BrdU^{+}$ cells amongst the retrovirus-uninfected cells (gfp^{-} cohort).

* indicates $p < 0.05$

A

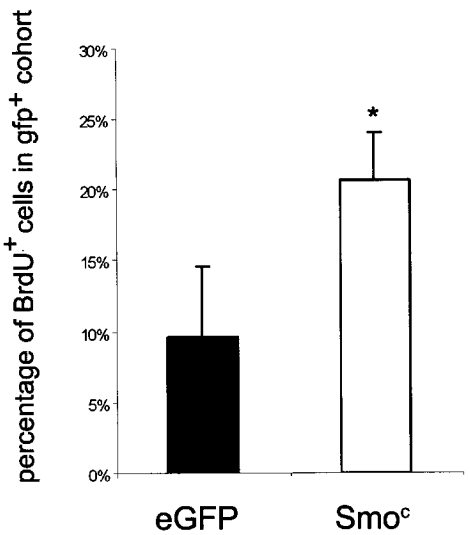
percentage of BrdU+ cells in gfp+ cohort
30%
25%
20%
15%
10%
5%
0%
*
eGFP
Smoc

B

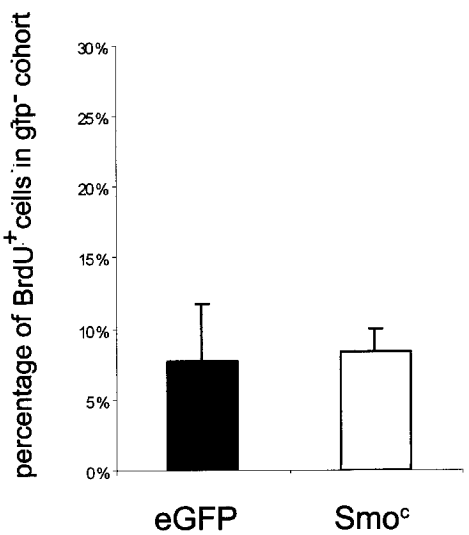
percentage of BrdU+ cells in gfp- cohort
30%
25%
20%
15%
10%
5%
0%
eGFP
Smoc

3.4 Cell-autonomous activation of the Hh signalling pathway promotes the differentiation of late-born INL cells at the expense of photoreceptor cells

To determine whether the constitutive activation of the Hh signalling pathway affects cell diversification of retinal precursor cells, we infected E18.5 mouse retina explants with Smo^{c}- or eGFP-retroviruses. Retinal explants were cultured for 10 days under the serum-free condition and then sectioned. By 10 days, the post-mitotic cells have completed migration and the three cellular layers can be distinguished in the explants: an inner RGC layer, a middle INL layer and an outer ONL layer *in vivo* (Fig. 2). However, in the retinal explant system, the RGC layer is devoid of RGCs at this stage, because RGC survival depends on trophic signals from their targets in the brain. As a consequence, RGCs die within 24 hours *in vitro* (30), but there are still some displaced amacrine cells in the RGC layer. Because I used retinal explants from E18.5 mice, I limited our analyses to the late-born cell types, such as rod photoreceptors, amacrine cells, bipolar cells and Müller cells, whose cell bodies are distributed between the INL and the ONL. We compared the distribution of gfp^{+} nuclei between the INL and the ONL in Smo^{c}- or eGFP-infected retinal explants. There was a 10% reduction and a corresponding 10% increase in Smo^{c}-infected cells in the INL and the ONL, respectively relative to eGFP-infected cells (Fig. 9). Thus, the cell-autonomous activation of the Hh signalling pathway had the tendency to promote the development of cells with an INL identity.

Figure 9. Distribution of retrovirus-infected cells in retinal layers.

E18.5 mouse retinal explants were infected with Smo^c- or eGFP-retroviruses, cultured for 10 days, and then were sectioned and processed for anti-GFP immunostaining. Proportions of infected cells in the INL and the ONL were compared.

p value indicates that there is no significant difference between Smo^c- and eGFP-retroviruses infected cells.

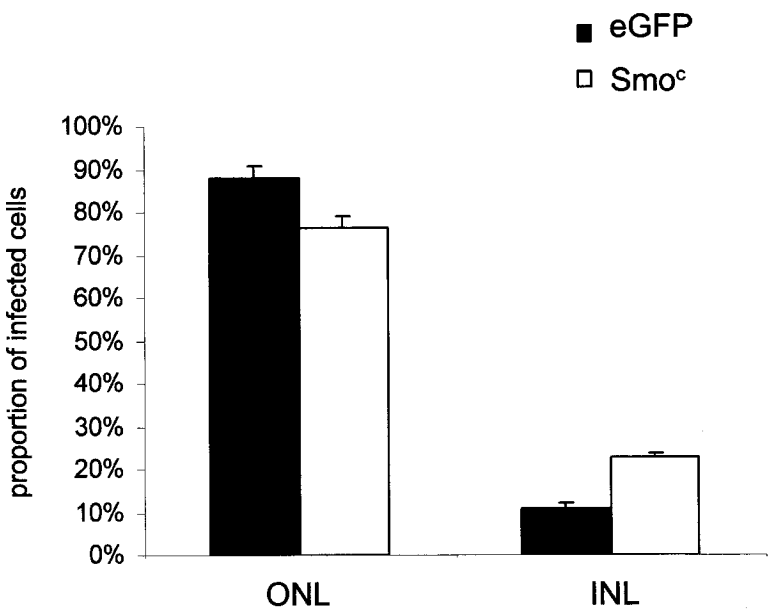
eGFP
Smo^c
100%
90%
80%
70%
60%
50%
40%
30%
20%
10%
0%
proportion of infected cells
ONL
INL

The cell distribution analyses of Smo^c-infected cells in explant sections indicated that Smo^c expression might promote the development of cells with an INL identity. To identify what types of cells were generated by Smo^c-infected RPCs, we dissociated the retrovirus-infected retinal explants after 10 days into single-cell suspensions and double stained with anti-GFP antibody and antibodies against cell type specific markers (Table 1 in Appendix B). We determined the proportions of cell marker-positive cells in the retrovirus-infected (gfp^+) and uninfected (gfp^-) cohorts by scoring the dissociated cells (Fig. 10). The proportions of Müller cells ($CRALBP^+$ cells), amacrine cells ($Pax6^+$ cells) and bipolar cells (PKC^+ cells) were increased by approximately two fold in the Smo^c-infected cells compared with the eGFP-infected cells (Fig. 11A); while the proportion of rod photoreceptors ($rhodopsin^+$ cells) was reduced by 3 fold in the Smo^c-infected cells compared with the eGFP-infected cells. This result was in agreement with the increase of the Smo^c-infected cells in the INL and the decrease of Smo^c-infected cells in the ONL. The changes in the proportion of INL cells were specific to the retrovirus-infected cohort, as the proportions of these cells were not different in the uninfected cohorts from the Smo^c- or eGFP-infected retinal explants. I did, however, observe a 20% reduction in the proportion of $rhodopsin^+$ cells in the uninfected cohort from Smo^c-infected retinal explants, indicating that Smo^c expression had a non-cell autonomous effect on rod photoreceptor development (Fig. 11B). The proportion of $nestin^+$ cells (precursor cells) was also increased by 3 fold in the Smo^c-infected cells compared with the eGFP-infected cells (Fig. 11A). The proportion of $nestin^+$ cells was unchanged among the uninfected cohort (Fig. 11B).

Figure 10. Examples of dissociated retinal cells stained with anti-GFP and cell specific markers.

E18.5 mouse retinal explants were infected with Smo^{c}- or eGFP-retroviruses and cultured for 10 days. After 10 days, retinal explants were dissociated into single cells and stained with anti-GFP antibody (green colour) and cell specific markers (red colour). Arrows indicate the double-stained cells (gfp^{+}/$marker^{+}$) and arrowheads indicate the gfp^{+}-only cells (gfp^{+}/$marker^{-}$).

Cell-type specific markers are listed on the left side of each row.

hoescht
cell marker
overlay
anti-CRALBP
anti-Pax6
anti-PKC
anti-nestin
anti-rhodopsin

Figure 11. Cell type analyses of retrovirus-infected retinal explants

E18.5 mouse retinal explants were infected with Smo^{c}- or eGFP-retroviruses and cultured for 10 days. After 10 days, retinal explants were dissociated to single cells and stained with anti-GFP antibody and cell specific markers. Müller cells were marked by anti-CRALBP antibody, amacrine cells were marked by Pax 6 antibody, bipolar cells were marked by PKC antibody and rod photoreceptors were marked by B630 antibody.

A. Quantification of different cell types amongst retrovirus-infected cells (gfp^{+} cohort).

B. Quantification of different cell types amongst retrovirus-uninfected cells (gfp^{-} cohort).

* indicates $p < 0.05$, ** indicates $p < 0.005$.

A

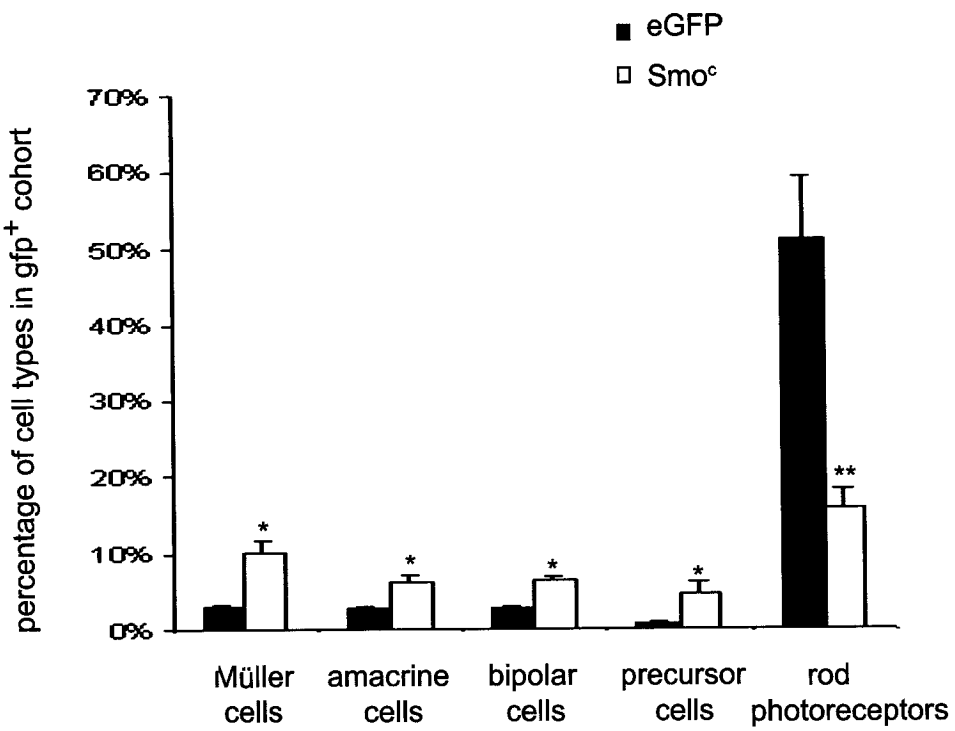
eGFP
Smo^c
70%
60%
50%
40%
30%
20%
10%
0%
percentage of cell types in gfp+ cohort
*
*
*
*
**
Müller cells
amacrine cells
bipolar cells
precursor cells
rod photoreceptors

B

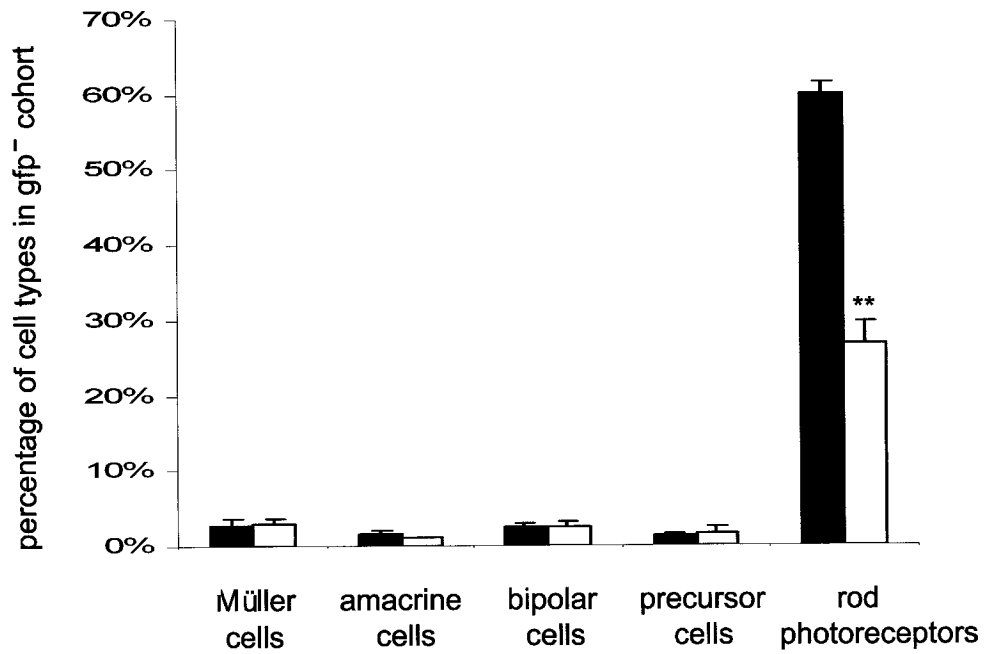
70%
60%
50%
40%
30%
20%
10%
0%
percentage of cell types in gfp- cohort
**
Müller cells
amacrine cells
bipolar cells
precursor cells
rod photoreceptors

3.5 Clonal analyses of retrovirus-infected retinal explants

Our results indicated that Smo^c expression promoted the development of cells destined for the INL, especially Müller glial. To see that effect *in situ*, I followed the progeny of single retrovirus-infected precursors (clones) by examining the size and constitution of the retrovirus-infected clones. The retinal explants cultured for 7 or 10 days under serum-free conditions had poor morphology that precluded my ability to accurately score the cellular distribution of clones. To circumvent this problem, I grew retinal explants in the presence of 10% FCS, which improved morphology. E18.5 retina explants were infected with the highly diluted Smo^c- or eGFP-retroviruses at the same titer of 10^6 CFU per ml, and then cultured for 7 days. After 7 days, the gfp-labeled cells were arranged in radial clusters (Fig. 12). A radial cluster of cells was considered to be a clone, i.e. derived from a single infected RPC. It was separated from the nearest gfp^+ radial cluster by at least four-cell diameters. The majority of clones were spaced further apart than 4 cell diameters. In Smo^c- or eGFP-infected clones, cells were distributed between the ONL and the INL. There were some clones whose nuclei were only located in the ONL (Fig. 13 A) or in the INL (Fig. 13B), while others contained cells spanning both layers (Fig. 14, 15).

The Smo^c-infected clones tended to be larger. The proportion of single-cell clones was 35% in Smo^c-infected clones compared with 70% of eGFP-infected clones, whereas the proportion of clones with more than 8 cells was 11% in Smo^c-infected clones, compared with 0.08% in eGFP-infected clones (Fig. 16).

Figure 12. A low-magnification view of retrovirus-infected clones

E18.5 mouse retinal explants were infected with Smo^{c}-retrovirus and cultured for 7 days in medium containing 10% FCS. After 7 days, retinal explants were sectioned at 8 μm and stained with anti-GFP antibody. The gfp-labeled cells were arranged in radial clusters, which were well separated from neighboring infected clones. Stars indicate a single retrovirus-infected clone.

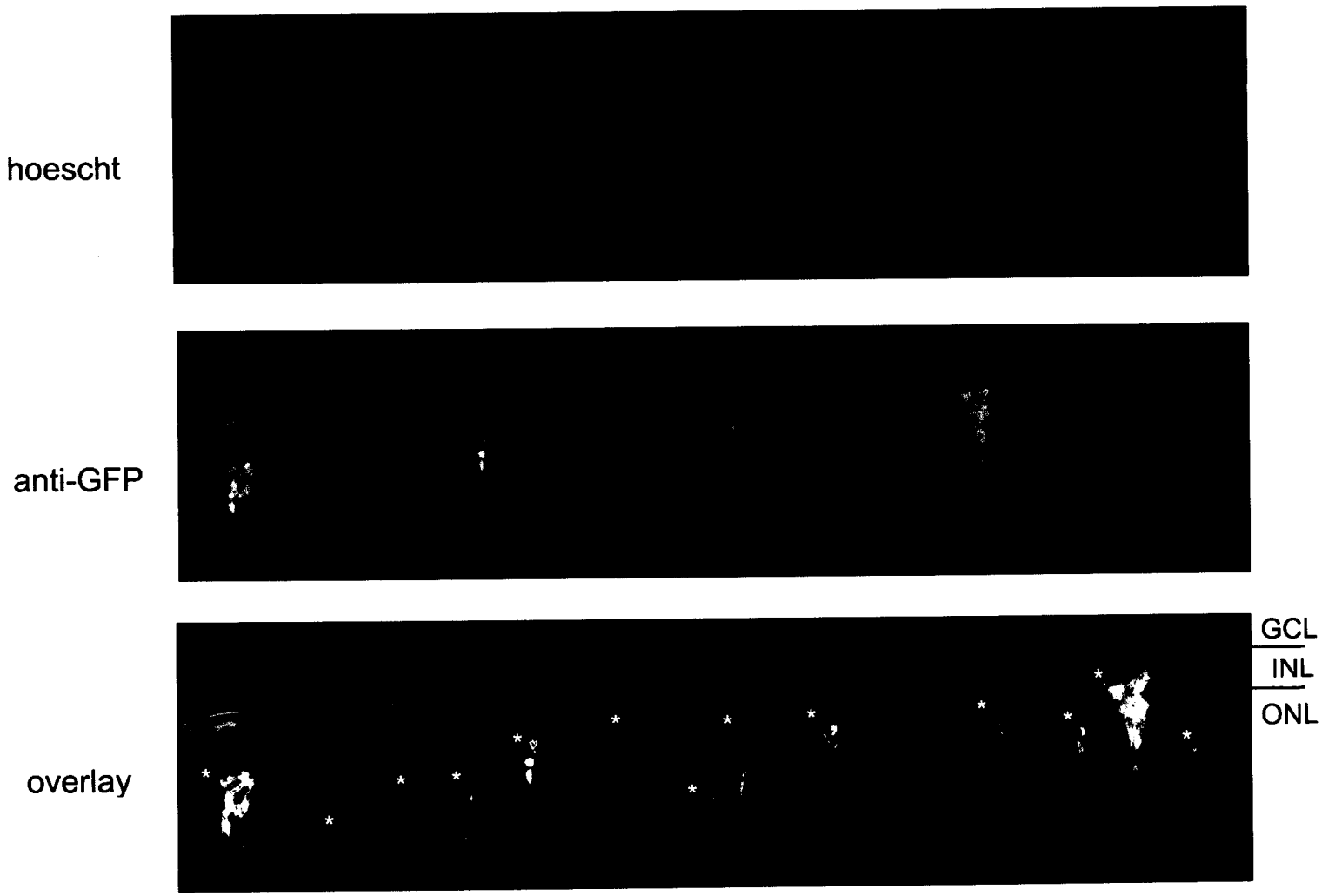
hoescht
anti-GFP
overlay
GCL
INL
ONL
40 μm

Figure 13. Examples of retrovirus-infected clones

E18.5 mouse retinal explants were infected with Smo^c-retroviruses and cultured for 7 days in medium containing 10% FCS. After 7 days, the retinal explants were sectioned at 8 μm and stained with anti-GFP antibody. Arrows indicate the cell bodies and arrowheads indicate the cell processes.

A. A clone with two cell bodies located in the ONL.

B. A clone with two cell bodies located in the INL.

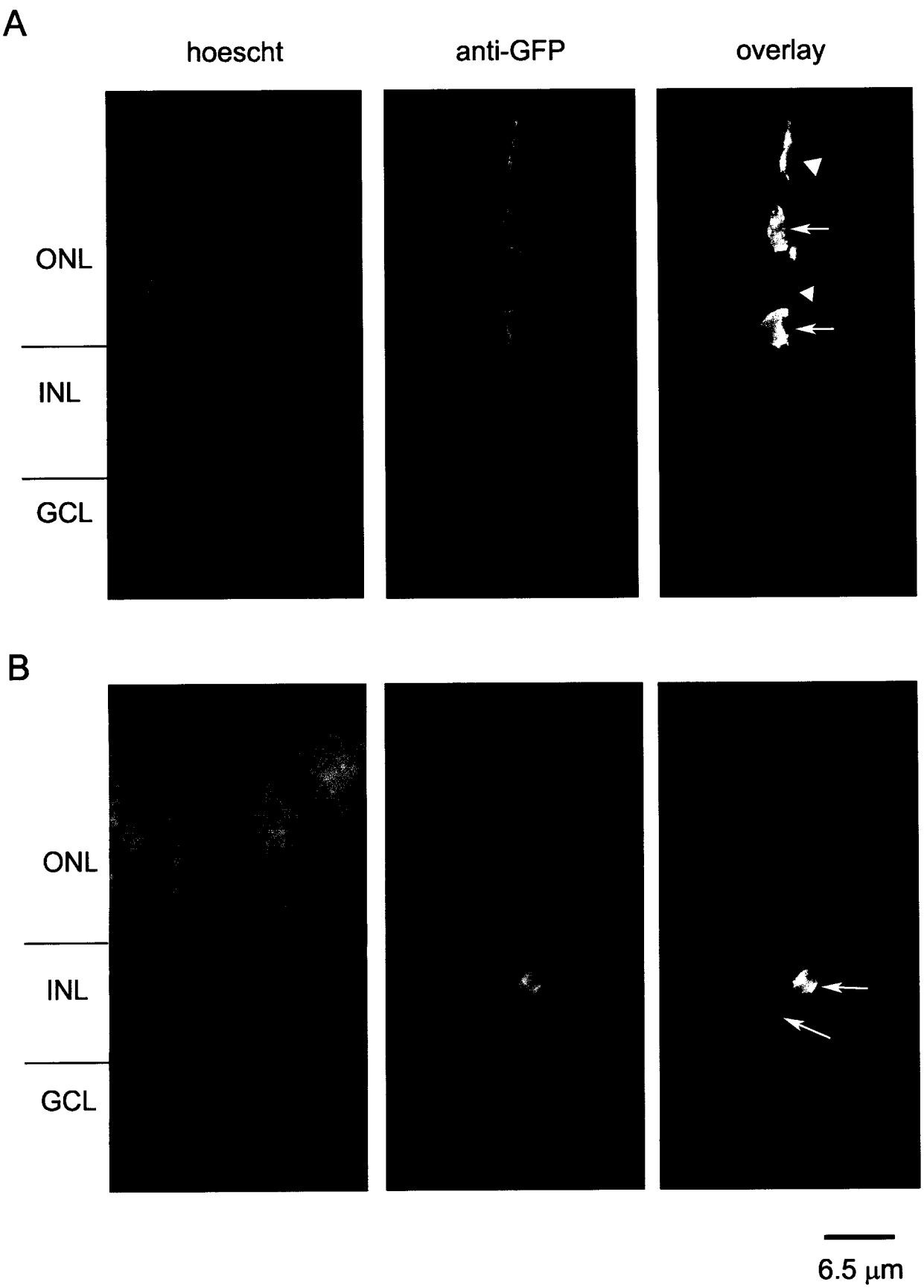
A
hoescht
anti-GFP
overlay
ONL
INL
GCL
B
ONL
INL
GCL
6.5 μm

Figure 14. An example of retrovirus-infected six-cell clone

E18.5 mouse retinal explants were infected with Smo^{c}-retroviruses and cultured for 7 days in medium containing 10% FCS. After 7 days, the retinal explants were sectioned at 8 μm and stained with anti-GFP antibody. Shown here is an example of a six-cell clone spanning ONL and INL, with 3 nuclei located in the ONL and 3 nuclei located in the INL. Arrows indicate the cell bodies, arrowheads indicate the cell processes and star indicates an end foot of a Müller glial cell.

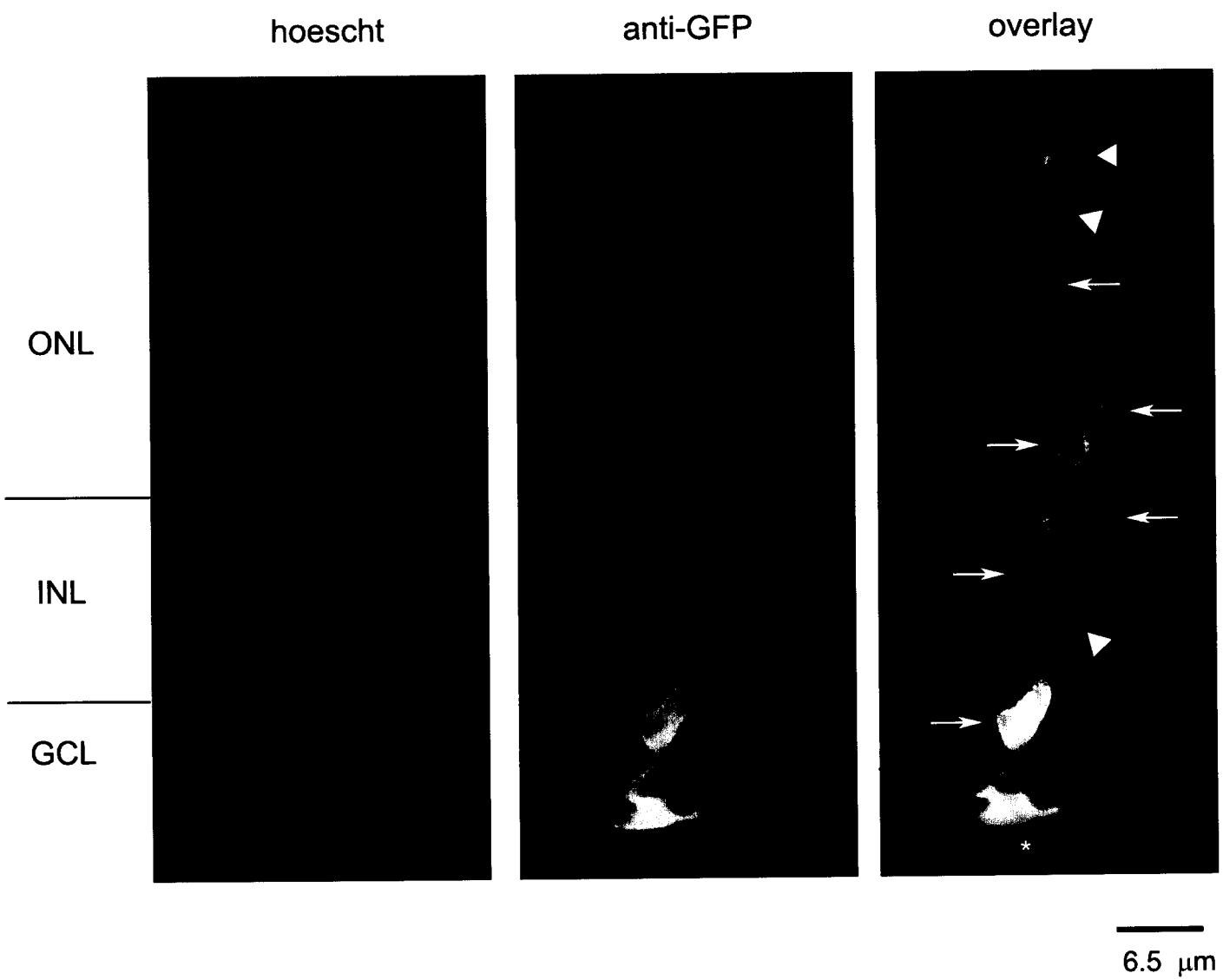
hoescht
anti-GFP
overlay
ONL
INL
GCL
6.5 μm

Figure 15. An example of a large retrovirus-infected clone

E18.5 mouse retinal explants were infected with Smo^c-retrovirus and cultured for 7 days in medium containing 10% FCS. After 7 days, retinal explants were sectioned at 8 μm and stained with anti-GFP antibody. Shown here is an example of a large clone. The exact number of cells was difficult to quantify.

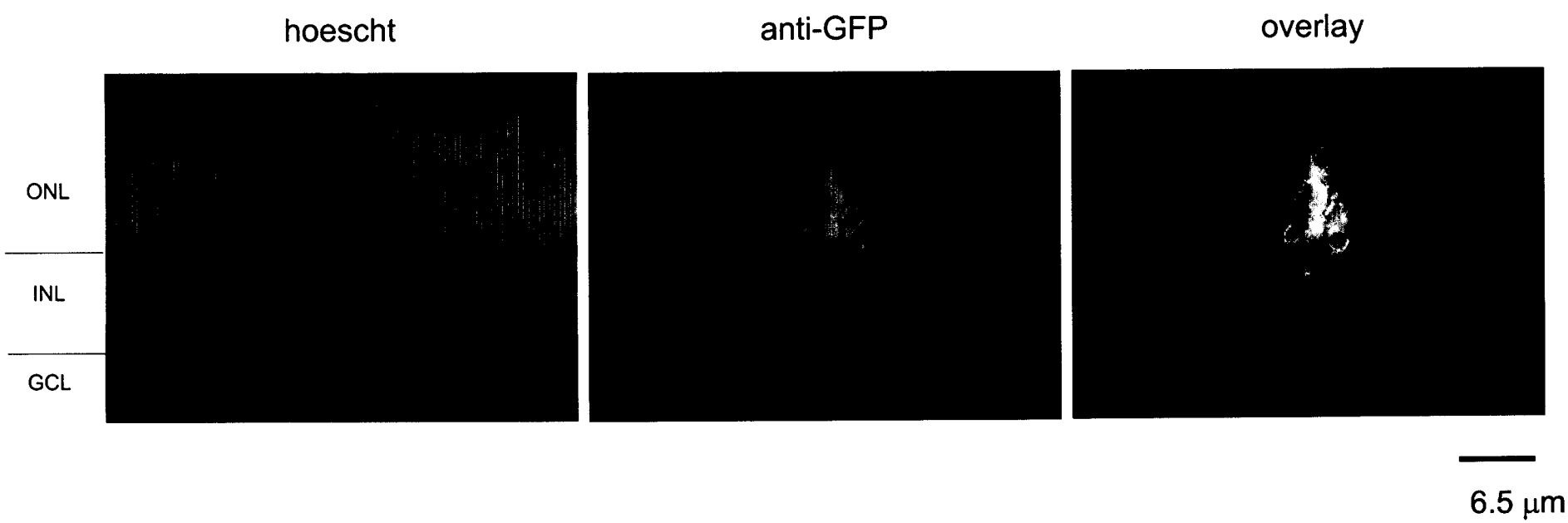
hoescht
anti-GFP
overlay
ONL
INL
GCL
6.5 μm

Figure 16. Comparison of clone size between Smo^c- and eGFP-retroviruses infected clones

E18.5 mouse retinal explants were infected with Smo^c- or eGFP-retroviruses and cultured for 7 days in medium containing 10% FCS. After 7 days, retinal explants were sectioned at 8 μm and stained with anti-GFP antibody. The retrovirus-infected clones were catalogued according to their size.

* indicates $p < 0.05$, ** indicates $p < 0.005$.

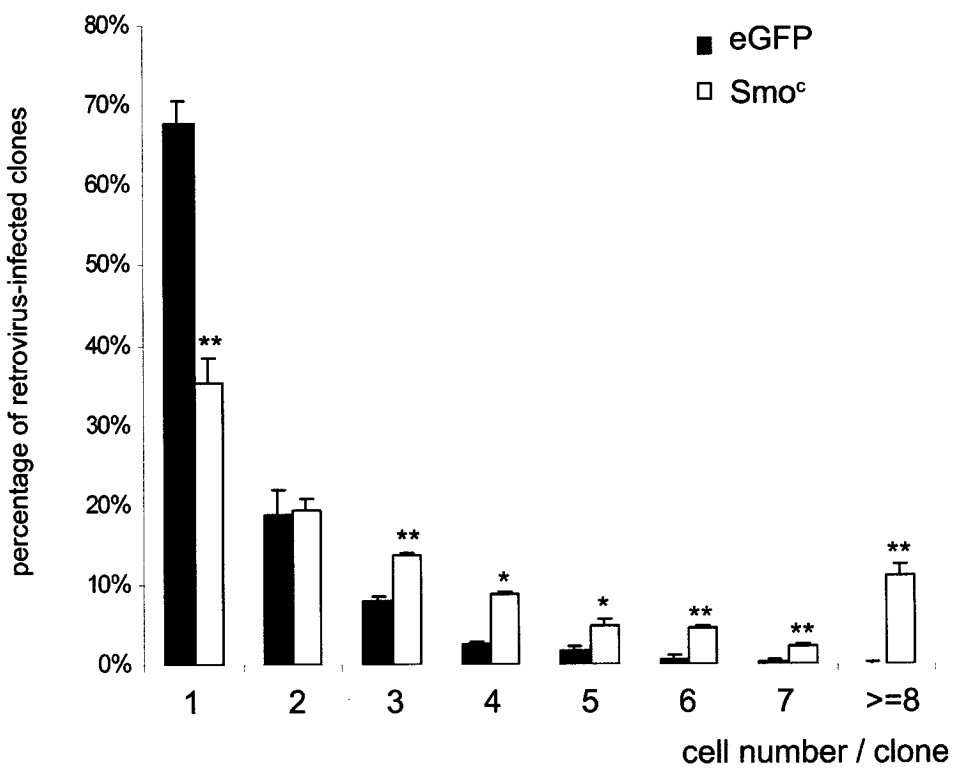
80%
70%
60%
50%
40%
30%
20%
10%
0%
percentage of retrovirus-infected clones
eGFP
Smo^c
**
**
*
*
**
**
**
1
2
3
4
5
6
7
>=8
cell number / clone

I also compared the distribution of nuclei in retrovirus-infected clones. After 7 days, the percentage of the clones spanning the ONL and the INL was increased 6 fold in Smo^c-infected clones compared with eGFP-infected clones, whereas there was a decrease of ONL cell-only clones in Smo^c-infected clones (Fig. 17).

Müller cells are the only progeny of RPCs that retain proliferative potential. Thus, it was possible that the increase in the percentage of Müller cells that we quantified by dissociated cell scoring amongst the Smo^c-infected cells could be secondary to an effect of Smo^c expression on Müller cell proliferation. If this were the case, I could have expected to see large Müller-cell-only clones. However, my clonal analyses did not reveal any exclusively Müller cell clones (Fig. 18). Therefore, the Smo^c- induced increase of Müller cell largely reflected a bias towards Müller cell development and not a proliferative effect.

Figure 17. Distribution of cells in retrovirus-infected clones

E18.5 mouse retinal explants were infected with Smo^c- or eGFP- retroviruses and cultured for 7 days in medium containing 10% FCS. After 7 days, retinal explants were sectioned at 8 μm and stained with anti-GFP antibody. The retrovirus-infected clones were catalogued according to the locations of cell nuclei between the INL and ONL.

* indicates $p < 0.05$.

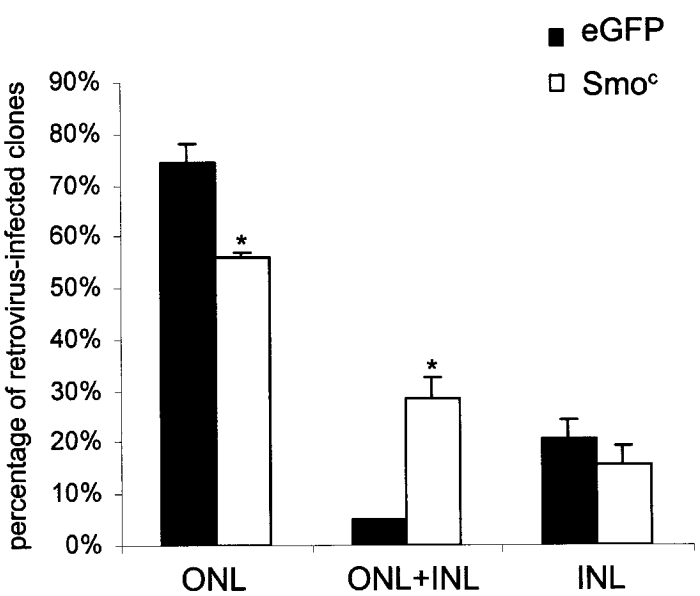
eGFP
Smo^c
percentage of retrovirus-infected clones
90%
80%
70%
60%
50%
40%
30%
20%
10%
0%
*
*
ONL
ONL+INL
INL

Figure 18. An example of a Smo^c-infected clone without exclusive Müller glia.

E18.5 mouse retinal explants were infected with Smo^c-retroviruses and cultured for 7 days in medium containing 10% FCS. After 7 days, retinal explants were sectioned at 8 μm and stained with anti-GFP and anti-CRALBP to detect Müller glia. Shown here is an example of a large Smo^c-infected clone that is not exclusively Müller glia cells.

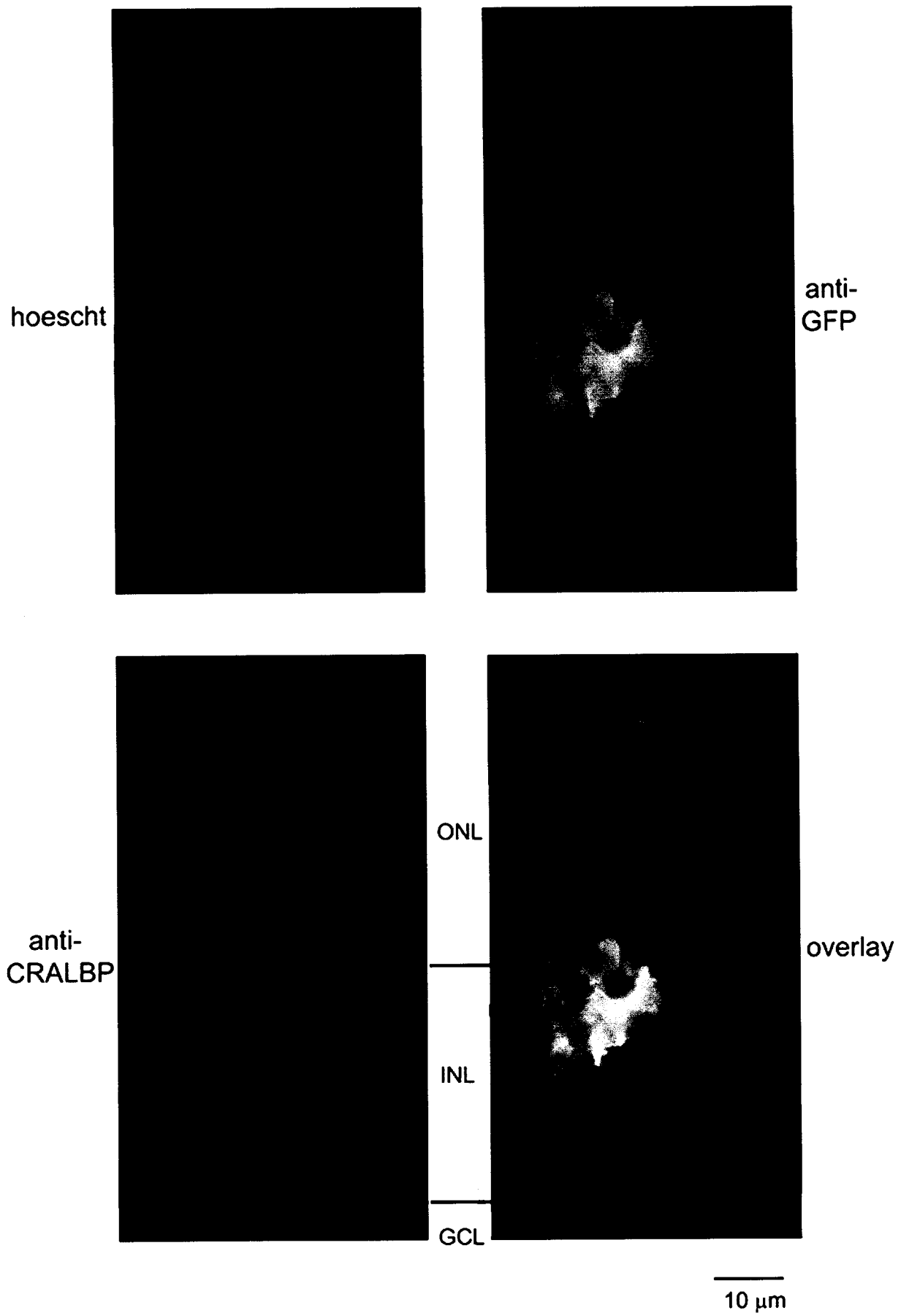
hoescht
anti-
GFP
anti-
CRALBP
ONL
INL
GCL
overlay
10 μm

3.6 Constitutive activation of the Hh signalling pathway inhibits the rhodopsin expression in rod photoreceptors

According to my results, Smo^c expression promoted the development of cells with an INL identity at the expense of cells with an ONL identity. Furthermore, the reduction of $rhodopsin^+$ cells in the uninfected cells from Smo^c-infected retinas indicated a non-cell autonomous effect of Smo^c expression on the development of rod photoreceptors. I therefore performed more extensive analyses of rod photoreceptor development in response to Smo^c expression. I infected E18.5 mouse retinas with Smo^c- or eGFP-retroviruses, cultured for 7 or 10 days, dissociated and stained with anti-GFP and anti-rhodopsin antibodies (Fig. 10). By 7 days, the proportion of $rhodopsin^+$ cells was decreased by 15% in Smo^c-infected cells compared with eGFP-infected cells (Fig. 19A). By 10 days, this difference was more pronounced (Fig. 19A). We also compared rhodopsin expression amongst the uninfected cohort of cells at two time points, 7 and 10 days, after infection. At 7 days, the proportion of $rhodopsin^+$ cells was not different in the uninfected cells from Smo^c- or eGFP-infected retinal explants; however, by 10 days, there was a two-fold decrease in the proportion of $rhodopsin^+$ cells in the uninfected cells from the Smo^c-infected retinal explants, compared with eGFP-infected explants (Fig. 19B). Thus, it seemed that the effects on the uninfected cells manifested late in the culture period.

I also examined rhodopsin staining in sections of the retrovirus-infected explants at 7 and 10 days of culture. At 7 days, there was no difference in the rhodopsin staining pattern in the Smo^c- or eGFP-infected retinal explants; in both cases, staining was continuous throughout the ONL and followed a central (highest) to peripheral (lowest) gradient, which is

consistent with the normal central to peripheral gradient of photoreceptor differentiation *in vivo* (Fig. 20), similar with the development of optic nerve, the exit point of RGC axon (99). By 10 days, however, the rhodopsin-staining pattern in the ONL in the Smo^c-infected explants was discontinuous, with positive regions interspersed with regions with reduced rhodopsin expression, even in the central region of the retinal explants; while the eGFP-infected explants exhibited a normal pattern of rhodopsin staining at 10 days (Fig. 21). The reduction of rhodopsin expression in the Smo^c-infected explants was not secondary to a change in cell survival, as there was no difference in TUNEL staining between the Smo^c-and eGFP-infected retinal explants (Fig. 22). The loss of rhodopsin expression did not correlate with an increase or difference in distribution of retrovirus-infected cells in those regions.

Figure 19. Rod photoreceptor cell scoring in retrovirus-infected retinal explants

E18.5 mouse retinal explants were infected with Smo^{c}- or eGFP-retroviruses and cultured for 7 and 10 days. After 7 or 10 days, retinal explants were dissociated to single cells and stained with anti-GFP and anti-rhodopsin antibodies and the proportion of $rhodopsin^{+}$ cells was quantified.

A. Quantification of $rhodopsin^{+}$ cells in retrovirus-infected (gfp^{+}) cohort.

B. Quantification of $rhodopsin^{+}$ cells in retrovirus-uninfected (gfp^{-}) cohort.

* indicates $p < 0.05$, ** indicates $p < 0.005$.

A

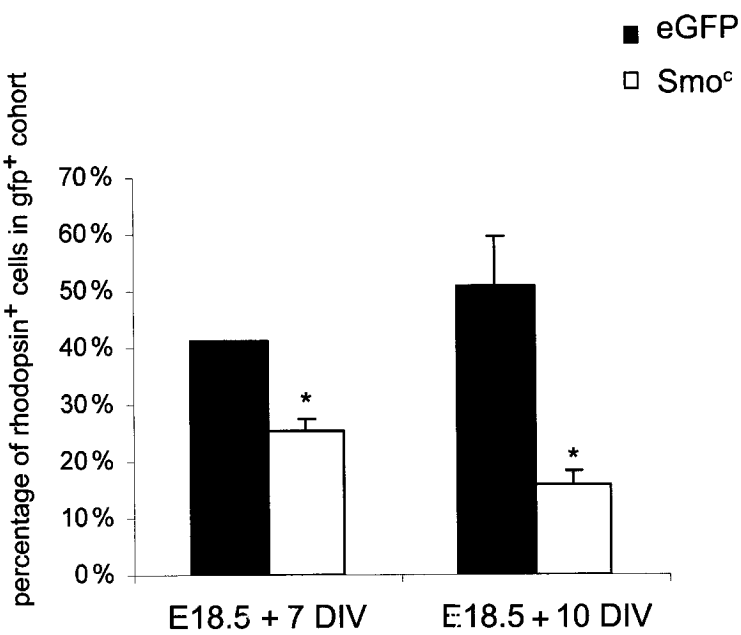
eGFP
Smo^c
percentage of rhodopsin+ cells in gfp+ cohort
70%
60%
50%
40%
30%
20%
10%
0%
*
*
E18.5 + 7 DIV
E18.5 + 10 DIV

B

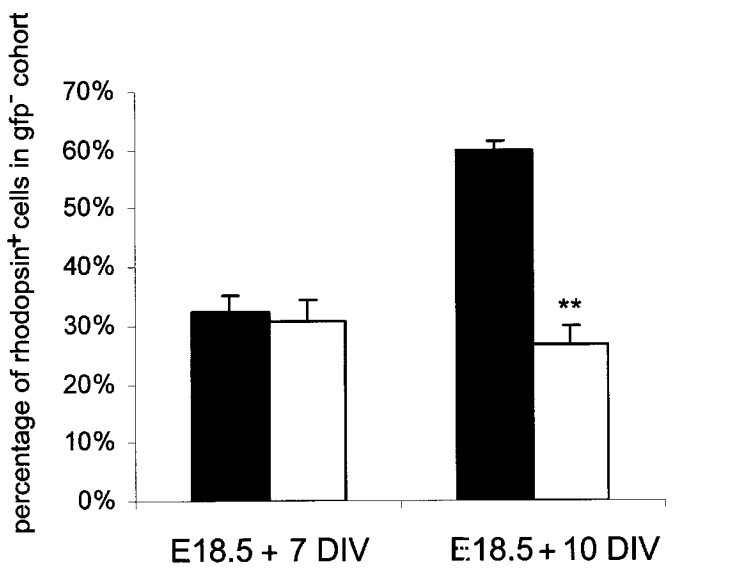
percentage of rhodopsin+ cells in gfp- cohort
70%
60%
50%
40%
30%
20%
10%
0%
**
E18.5 + 7 DIV
E18.5 + 10 DIV

Figure 20. Rhodopsin staining pattern in retrovirus-infected retinal explants at 7 days *in vitro*.

E18.5 mouse retinal explants were infected with Smo^c- or eGFP-retroviruses and cultured for 7 days. After 7 days, retinal explants were sectioned at 8 μm and stained with anti-GFP and anti-rhodopsin antibodies. The rhodopsin-staining pattern in the ONL was the same between Smo^c- and eGFP-infected retinal explants: continuous, decreased in gradient from central region (highest) to peripheral region (lowest) of retinal explants, similar with the development of optic nerve, the exit point of RGC axon.

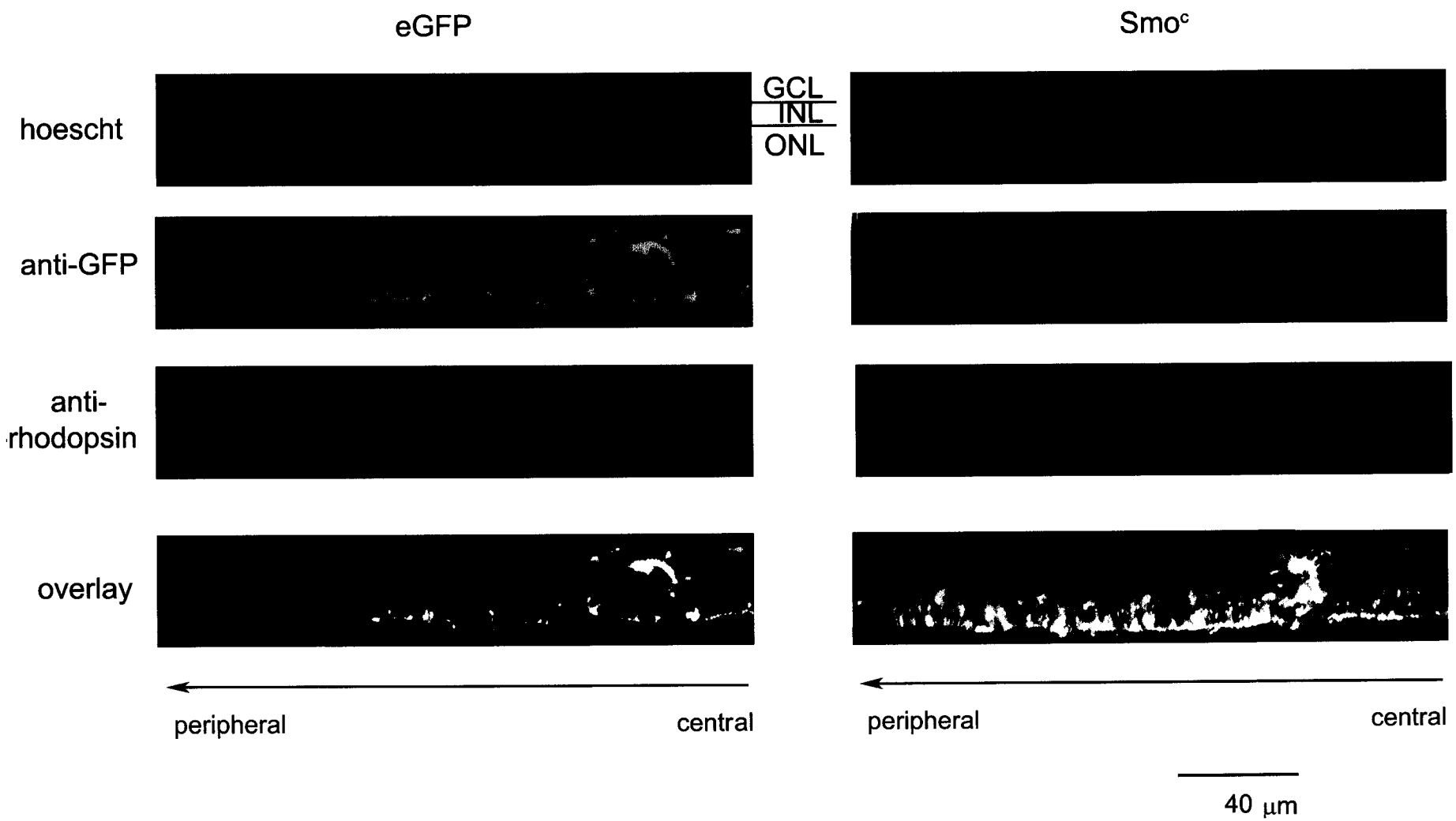
eGFP
Smo^c
hoescht
anti-GFP
anti-
rhodopsin
overlay
GCL
INL
ONL
peripheral
central
peripheral
central
40 μm

Figure 21. Rhodopsin staining pattern in retrovirus-infected retinal explants at 10 days *in vitro*

E18.5 mouse retinal explants were infected with Smo^c- or eGFP-retroviruses and cultured for 10 days. At 10 days, retinal explants were sectioned at 8 μm and stained with anti-GFP and anti-rhodopsin antibodies. The rhodopsin-staining pattern in the ONL in Smo^c-infected retinal explants was discontinuous, with positive regions interspersed with regions with reduced rhodopsin expression, even in the central region of the retinal explants; eGFP-infected retinal explants exhibited a normal pattern of rhodopsin staining. Arrows indicate the $rhodopsin^-$ regions in the Smo^c-infected retinal explants.

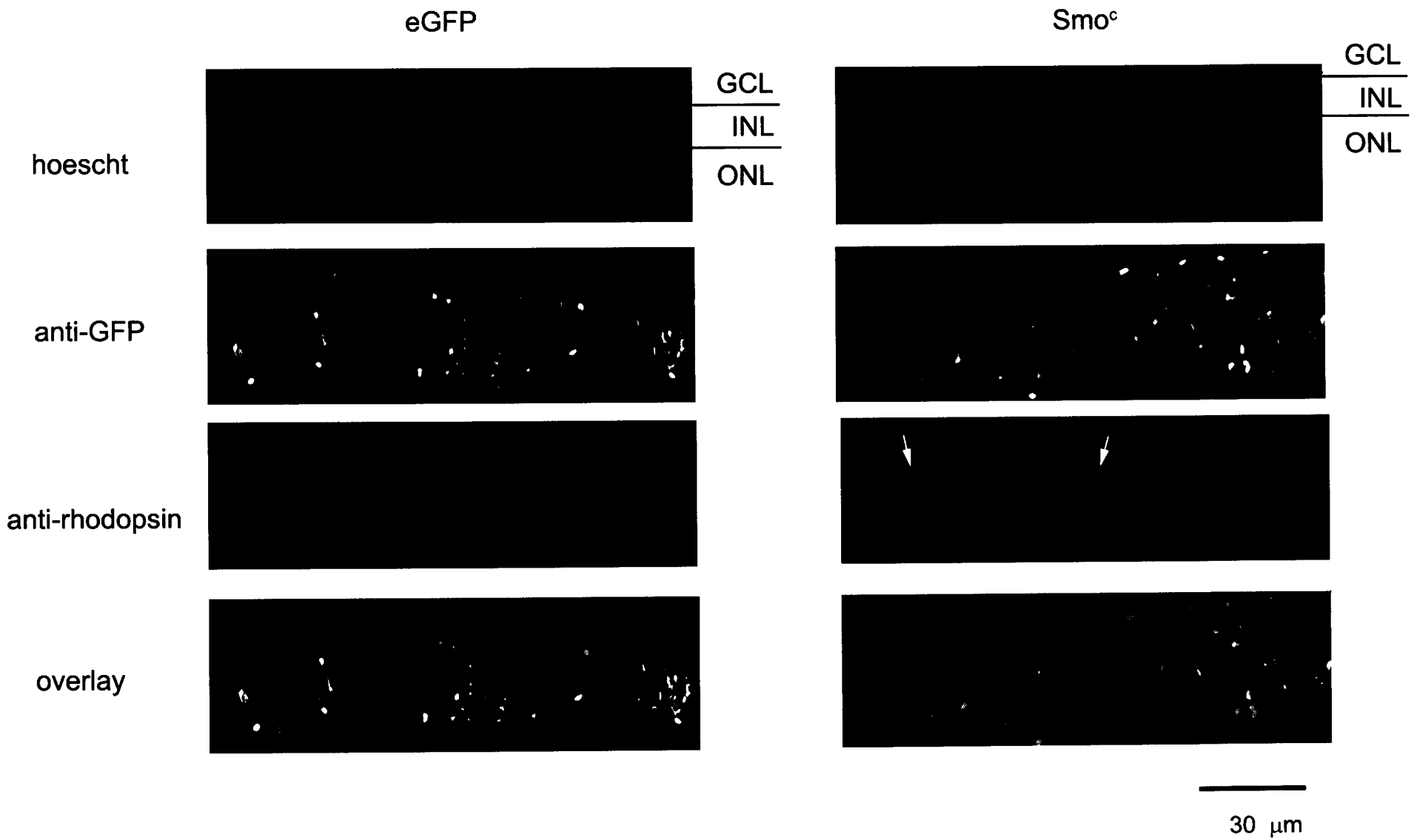
eGFP
Smo^c
GCL
INL
ONL
hoescht
anti-GFP
anti-rhodopsin
overlay
30 μm

Figure 22. TUNEL staining in retrovirus-infected retinal explants at 10 days *in vitro*

E18.5 mouse retinal explants were infected with Smo^c- or eGFP-retroviruses and cultured for 10 days. After 10 days, retinal explants were sectioned at 8 μm and apoptotic cells were stained by TUNEL. There was no qualitative difference in the presence of apoptotic cells between the Smo^c- and the eGFP-infected retinal explants.

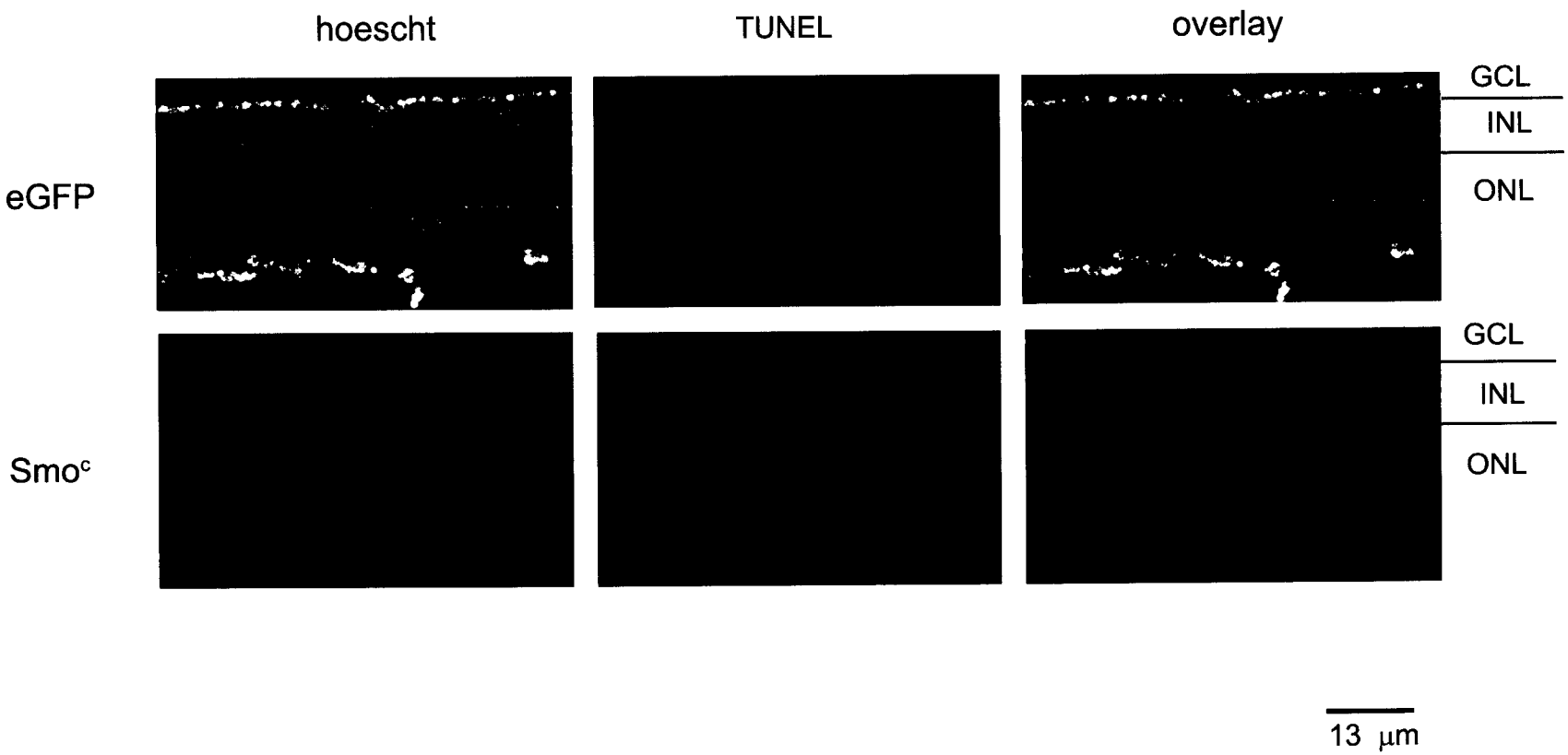
hoescht
TUNEL
overlay
eGFP
Smo^c
GCL
INL
ONL
GCL
INL
ONL
13 μm

To determine whether the reduction in rhodopsin expression in Smo^c-infected retinal explants represented a general reduction in rod photoreceptor specification or differentiation, I looked at an additional marker of rod development, nuclear morphology. Rods exhibit characteristic nuclear morphology: small nuclei with one or more large clumps of heterochromatin (32) (Fig. 23). The proportion of cells with characteristic rod nuclear morphology was reduced by 30% in the Smo^c-infected cells compared with the eGFP-infected cells (Fig. 24A), suggesting that fewer cells are specified as rods among the Smo^c-infected cohort of RPCs. However, the percentage of cells with characteristic rod nuclear morphology was not significantly reduced among the uninfected cohort in Smo^c-infected explants (Fig. 24B), suggesting that rods were specified, but that expression of Smo^c in neighbouring cells interferes with rhodopsin expression.

Two additional markers, CRX and recoverin, are expressed in rod photoreceptors prior to rhodopsin expression. CRX is a homeodomain transcription factor, which is expressed exclusively in rod and cone photoreceptors and is induced soon after terminal mitosis (39). I examined *CRX* expression by *in situ* hybridization on explant sections harvested at 7 and 10 days of culture. There was no significant difference in the expression pattern of *CRX* between the Smo^c- and the eGFP-infected explants (Fig. 25). Recoverin staining represents an earlier readout of the inhibitory effects of Smo^c-infected cells on rod photoreceptor differentiation (95). After 10 days, the retrovirus-infected retinal explants were dissociated into single cells and stained with anti-GFP and anti-recoverin antibodies (Fig. 26). There was a similar reduction of recoverin expression in the uninfected cohort from Smo^c-infected explants (Fig. 24A, B), although this difference was smaller compared to the reduction of rhodopsin expression in the uninfected cohort from the Smo^c-infected explants.

Figure 23. Nuclear morphology of rod photoreceptors

E18.5 mouse retinal explants were infected with Smo^{c}-retroviruses and cultured for 10 days. At 10 days, retinal explants were dissociated into single cells and stained with anti-rhodopsin antibody. Rods have the characteristic nuclear morphology: smaller nuclei than other retinal cell types, with one or more large clumps of heterochromatin.

All of the arrowhead- and arrow-marked cells exhibit a similar nuclear morphology, but with or without rhodopsin staining and are all scored as rod photoreceptors. Arrowheads indicate $rhodopsin^{+}$ cells and arrows indicate the $rhodopsin^{-}$ cells that exhibit a rod nuclear morphology. While stars point out the nucleus of the non-rod cells, which are bigger, dimmer in the nucleus or have no large clumps of heterochromatin.

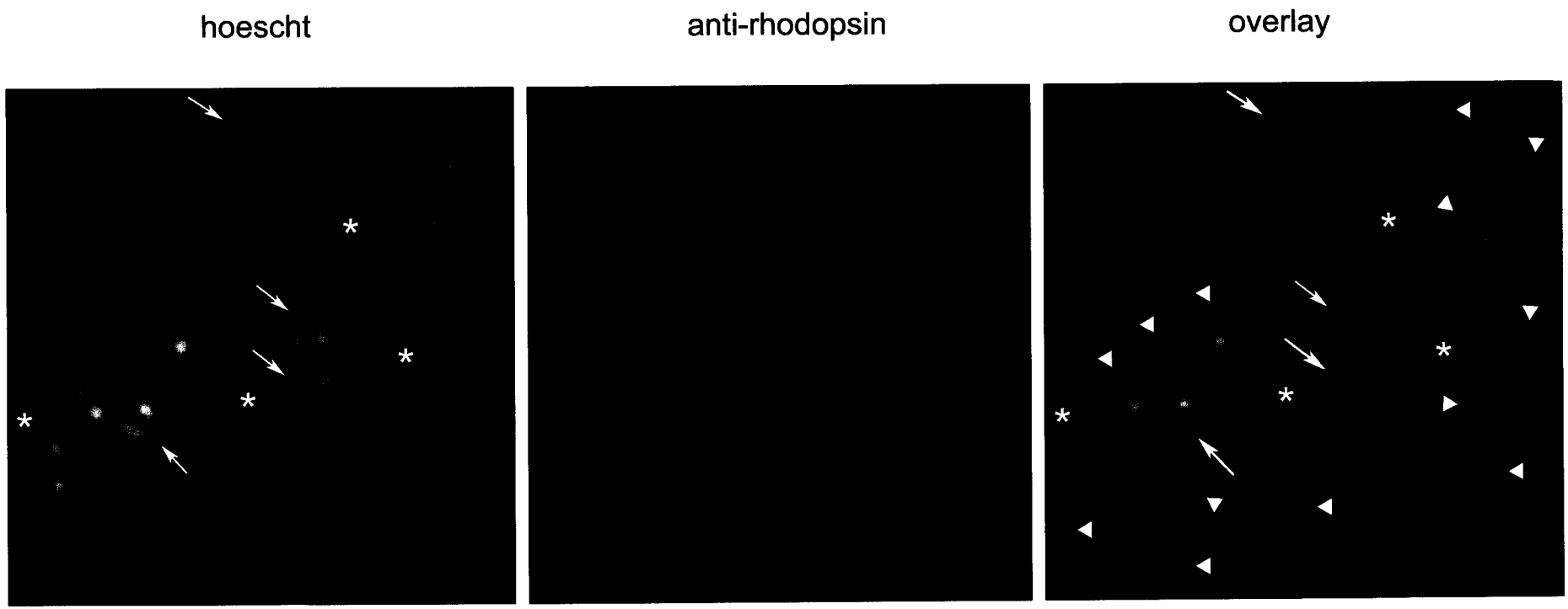
hoescht
anti-rhodopsin
overlay

Figure 24. Quantification of rod photoreceptors

E18.5 mouse retinal explants were infected with Smo^{c}- or eGFP-retroviruses and cultured for 10 days. At 10 days, retinal explants were sectioned at 8 μm, dissociated into single cells and stained with anti-GFP, anti-rhodopsin or anti-recoverin antibodies. The proportions of $marker^{+}$ cells or cells in a rod nuclear morphology were quantified.

A. Quantification of rod photoreceptors in the retrovirus-infected (gfp^{+}) cells.

B. Quantification of rod photoreceptors in the retrovirus-uninfected (gfp^{-}) cells.

* indicates $p < 0.05$, ** indicates $p < 0.005$.

A

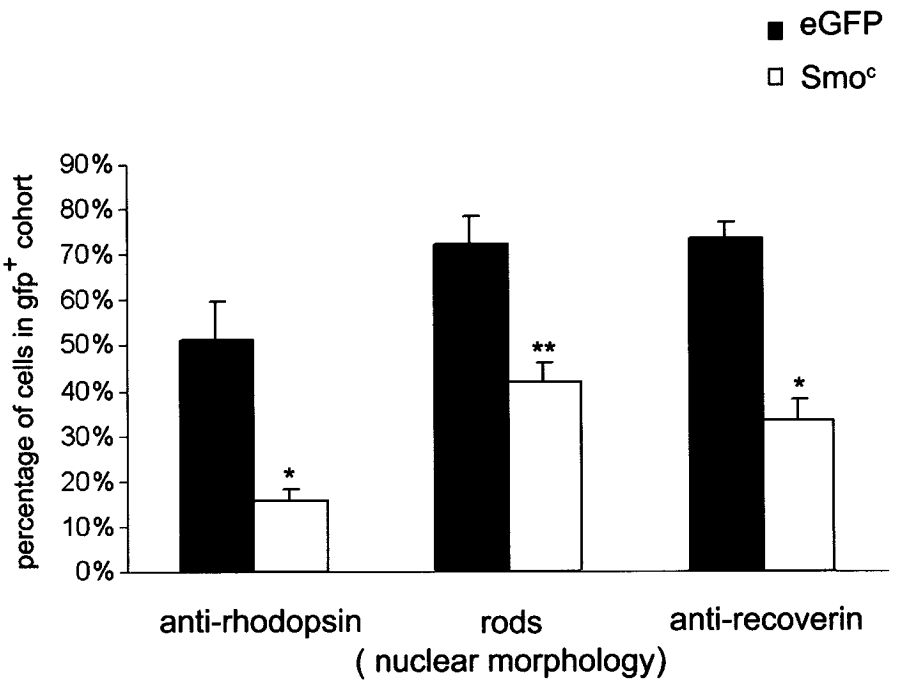
eGFP
Smo^c
percentage of cells in gfp+ cohort
90%
80%
70%
60%
50%
40%
30%
20%
10%
0%
*
**
*
anti-rhodopsin
rods
anti-recoverin
(nuclear morphology)

B

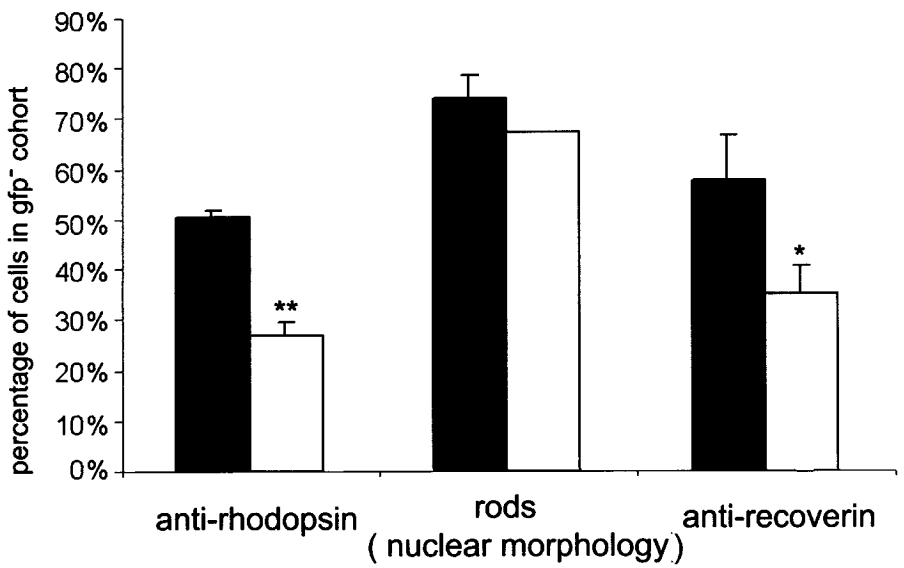
percentage of cells in gfp- cohort
90%
80%
70%
60%
50%
40%
30%
20%
10%
0%
**
*
anti-rhodopsin
rods
anti-recoverin
(nuclear morphology)

Figure 25. *CRX* expression pattern

E18.5 mouse retinal explants were infected with Smo^c- or eGFP-retroviruses and cultured for 7 or 10 days. At 7 or 10 days, retinal explants were sectioned at 12 μm and performed *in situ* hybridization with *CRX* probe. There was no significant difference between the Smo^c- and the eGFP-infected retinal explants in both periods.

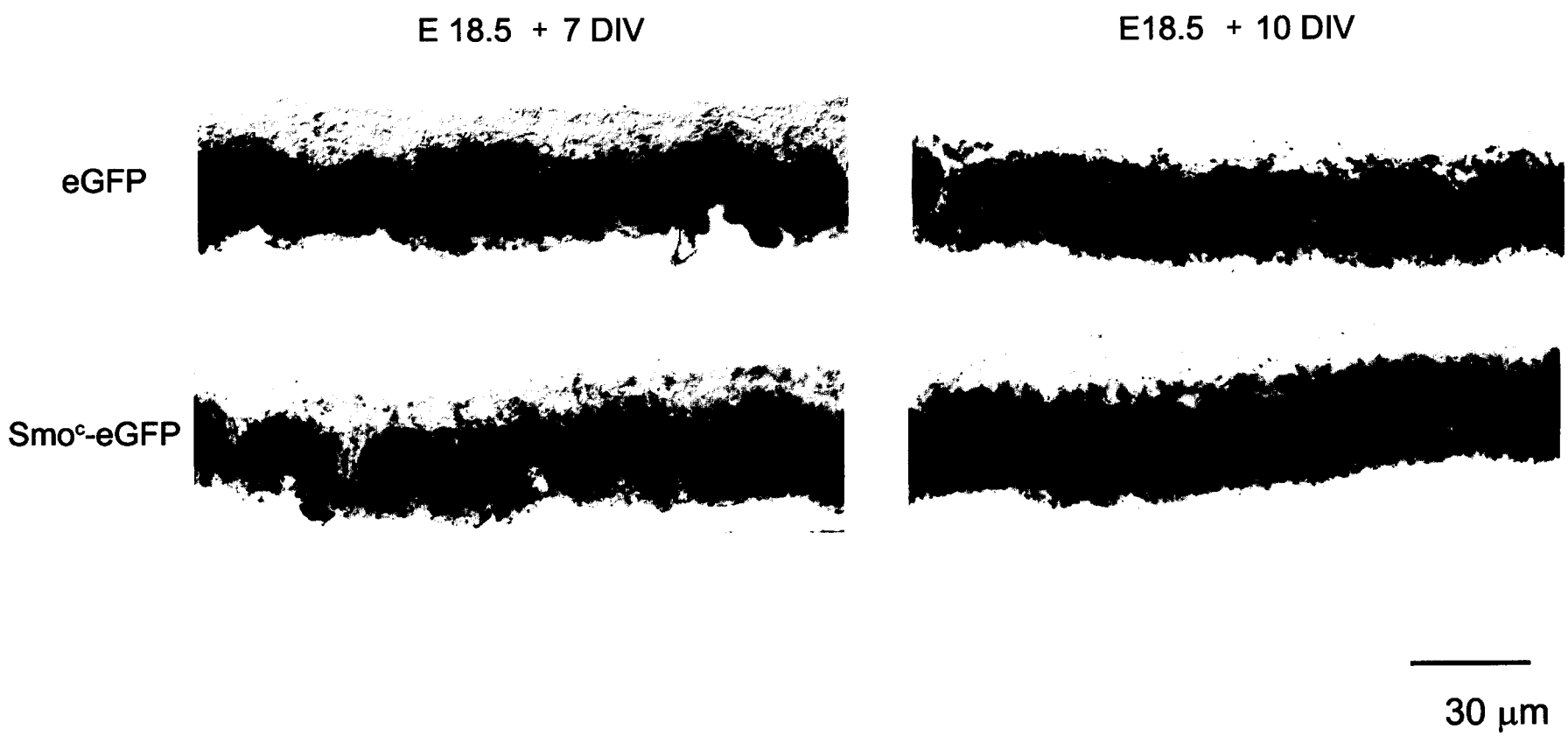
E 18.5 + 7 DIV
E18.5 + 10 DIV
eGFP
Smo^c-eGFP
30 μm

Figure 26. Examples of dissociated retinal cells stained with anti-GFP and anti-recoverin antibodies

E18.5 mouse retinal explants were infected with Smo^{c}- or eGFP-retroviruses and cultured for 10 days. After 10 days, retinal explants were dissociated into single cells and stained with anti-GFP (green colour) and anti-recoverin (red colour) antibodies.

Arrow indicates a double-stained cell (gfp^{+} / $recoverin^{+}$) and arrowheads indicate gfp^{+}-only cells (gfp^{+} / $recoverin^{-}$).

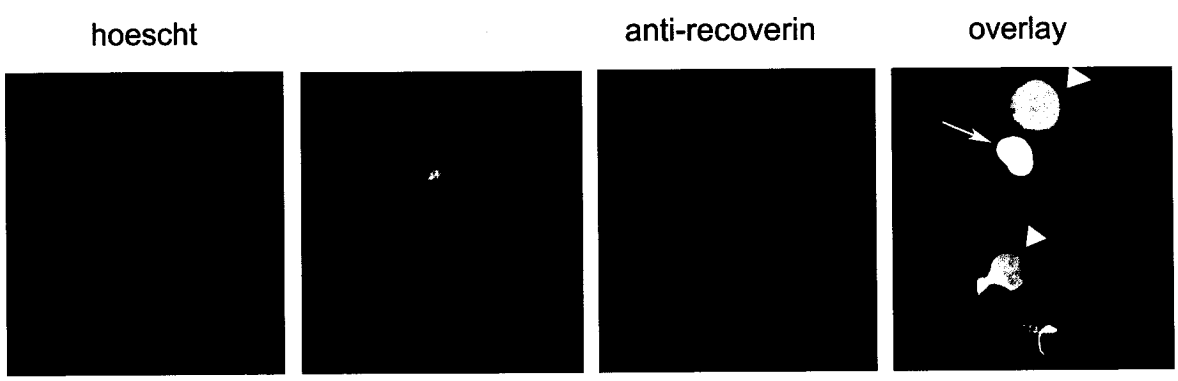
hoescht
anti-recoverin
overlay

Now this is not the end. It is not even the beginning of the end. But it is, perhaps, the end of the beginning.

- Sir Winston Churchill (1874 - 1965), Speech in November 1942

Discussion

We observed that the activation of the Hh signalling pathway, driven by the expression of Smo^c, has two types of effects in mouse perinatal retinal explant cultures. The first is a cell-autonomous effect whereby the effects of Smo^c expression were only measurable in the infected cells. Thus, Smo^c expression promoted RPC proliferation, increased progenitor cell number, and promoted the development of INL cells at the expense of photoreceptors. The second is a non-cell autonomous effect, where the presence of Smo^c-infected cells exerted effects on uninfected cells. In this instance, Smo^c expression caused a decrease in rhodopsin expression amongst the uninfected cohort of cells in the retinal explants.

4.1 The activation of Hh signalling pathway driven by Smo^c

Smo^c can escape inhibition by Ptc and mimic the effects of the Hh signal *in vivo* and *in vitro*. Smo^c expression activated the Hh signalling pathway in C3H 10T1/2 cells by up-regulating *Gli1* expression. Expression of Smo^c in *Xenopus* embryos leads to developmental anomalies that are consistent with known requirements for Hh signalling in the *Xenopus* eye (100). Ectopic Smo^c expression has been used to examine the effects of cell autonomous Hh signalling pathway activation in other tissues. In order to inspect the patterning mechanism in the developing neural tube, Hynes et al. expressed the same activating form of Smo^c to the developing neural tube and found that it mimicked the actions of Shh signal to activate differentiation of precursor cells, inducing the cell types requiring high concentrations of Shh that develop adjacent to Shh-producing floor plate and notochord cells, as well as cell types induced by low concentrations of Shh that develop at a distance from the Shh source (82).

Each of the examined cell types were induced cell autonomously in Smo^c-expressing cells but not in adjacent or distant cells (82). Transgenic expression of wild type Smo did not have the same effects (82), indicating that ectopic expression of wild-type Smo is still antagonized by Ptc.

Combining the facts that Smo^c expression constitutively activates the Hh signalling pathway and the effects of Hh signalling pathway on retina development, I expected that ectopic expression of Smo^c in the developing mouse retina explants would constitutively activate Hh signalling and then promote RPC proliferation and differentiation.

4.2 The Hh signalling pathway is essential for the proliferation of mouse retinal precursors

The Hh signal is one of the known mitogens that promote the proliferation of precursor cells in the CNS (98). There is strong *in vivo* and *in vitro* evidence that Shh drives RPC proliferation in the retina (31, 101). The evidence of *in vivo* proliferation controlled by the Hh signalling pathway is provided by the fact that the Shh conditional knockout mice have smaller eyes (30), a reduction in cyclin D expression, and a decrease in the percentage of dividing cells (unpublished data from our lab). Shh also promotes proliferation of RPCs in the developing mouse retinal explants and dissociated cells (31). The above observations are consistent with our results: there was an increase in the proportion of $BrdU^+$ cells and $nestin^+$ cells in the Smo^c-infected RPCs, indicating that there were more S-phase cells and precursor cells. This promotion of RPC proliferation driven by the Smo^c expression acted in a cell autonomous way, as there was no effect on the proliferation of uninfected cells. The

increased proportion of nestin$^+$ cells in the Smo^c-infected cohort at 7 days suggested that Smo^c expression might have inhibited differentiation of RPCs. Nestin is present in the neuroepithelial stem cells, probably marking the earliest neuron precursor cells (98). Alternatively, these nestin$^+$ cells in the Smo^c-infected cohort could also be Müller glia, as Müller glia express nestin (99). This is also consistent with my observation that Smo^c expression promoted Müller glia development.

It is clear that the Shh signalling pathway can affect several cell-cycle parameters. Shh signalling pathway drives continued cycling in immature, proliferating cerebellar granule neuron precursors (CGNPs) by promoting the expression of N-myc which up-regulates D-type cyclin gene expression (101). Shh also induces dramatic increases in the proportion of actively proliferating cells within stratified epithelium by inhibiting p21, an inhibitor of CDK activity, which leads to Rb phosphorylation in epithelial cells (102). However, Shh promotes the expression of cyclin D1, not N-myc, in the developing mouse retina (unpublished data from our lab), so it is not clear how it is driving cyclin D1 expression in the mouse retina. Thus, it is worth looking at the changes in the expression of these genes in Smo^c-infected cells to see if cell autonomous activation of Shh signalling pathway is sufficient to mediate all of these effects on cell cycle.

4.3 The Hh signalling pathway promotes the differentiation of RPCs into INL cells at the expense of rod photoreceptors

I focused on the differentiation of RPCs at the perinatal period during mouse retinal development. The results showed that Smo^c expression promoted the differentiation of the

late-born INL cells --- Müller glia, bipolar cells and amacrine cells at the expense of rod photoreceptors in a cell-autonomous way.

Modulation of the Hh signalling pathway has been shown to affect cell diversification in the retina. Recombinant Shh-N promotes an increase in rod photoreceptors, amacrine and Müller cells in the mouse retinal aggregate or pellet cultures (31). Conversely, blockade of the Hh signalling pathway by injection of antisense oligonucleotides against *Shh* and *twhh* reduces and delays photoreceptor differentiation in zebrafish (103). While, these findings are consistent with my observation that Smo^c expression promoted INL cell development, they are difficult to reconcile with our findings that Smo^c expression had a negative effect on rod photoreceptor development. These discrepancies could reflect effects of different culture conditions (pellet versus explant cultures), different methods of the Hh signalling pathway activation (recombinant protein versus retrovirus) and different species (mouse versus fish). Furthermore, among the cell types I counted, the decrease of rod photoreceptors was balanced with the increases of the late-born INL cells.

It is not clear how the Hh signalling pathway promotes Müller glia and bipolar cell development. One possibility is that it may modulate *Hes 1* expression. *Hes 1* is a basic helix-loop-helix (bHLH) gene and *Hes 1*-null animals exhibit premature retinal neuron differentiation and a reduction in Müller glia and bipolar cell development, whereas misexpression of *Hes 1* promotes Müller glia development at the expense of rod photoreceptors (104) (38). Since we found that *Hes 1* was up-regulated in the Shh-N treated retinal explants (unpublished data from our lab), there was a possibility that Hes 1 was also involved in the differentiation of RPCs driven by the Smo^c expression. Thus, it would be interesting to determine whether the Müller glia-promoting effect of the Smo^c expression requires Hes 1 expression.

Since RPC proliferation and differentiation are intertwined temporally during retinal development, how these two processes are co-ordinated is an important question. So far, little is known about how this coordination proceeds. Smo^c expression could promote INL cell development via maintaining RPCs in cell cycle until they reach a stage where they are intrinsically competent to differentiate as INL-type cells. Alternatively, Smo^c expression may act intrinsically to bias RPCs towards INL cell fates at the expense of rod photoreceptors. Based on how I performed these experiments, I cannot distinguish between these two possibilities.

The RGC-derived Shh signal is required for the lamination of mouse retina both *in vitro* and *in vivo* (30). In mouse retina explant cultures, recombinant Shh-N treatment prompts normal photoreceptor morphology and the development of a radial scaffold of Müller glia (30), which is important for the maintenance of the retinal lamination (105). In conditional *Shh* knockout mice, the lamination defects of the retina are observed at E17, consistent with the onset of differentiation of Müller glia (30). Ectopic Shh expression in small clones of cells in the retina of *Shh* mutant zebrafish promotes normal lamination of adjacent, mutant retinal tissue, indicating that the *Shh*-expressing cells exert a short-range effect on their neighbours to restore retinal lamination (106). In contrast, ectopic expression of Smo^c did not have a dramatic effect on retinal lamination, as there was extensive rosetting in the ONL in Smo^c–infected explants. It is possible that for the Hh signalling to restore lamination, it must act directly over several cell diameters, which would be the case when Shh, but not Smo^c, is expressed. Finally, it is possible that the Hh signalling pathway activation via Smo^c does not mimic all of the effects of the Hh ligand. For example, Shh has been shown to alter adhesiveness of neuroepithelial cells in a manner that is independent of signalling through the Ptc/Gli axis (107).

4.4 The Hh signalling pathway inhibits rod photoreceptors from expressing rhodopsin in a non-cell autonomous way

I also observed non-cell autonomous effects of the constitutive activated Hh signalling pathway on retinal cell development. At 10 days, rhodopsin expression was decreased by two fold in the uninfected cohort from the Smo^c-infected retinal explants in the presence of approximately 5% Smo^c-infected cells. The negative effects on bystander rhodopsin expression initiated by the Smo^c expression was unlikely a secondary effect of viral infection or load of uninfected cells, as the percentage of infected cells in Smo^c- and eGFP-infected retinal explants was not significantly different at 10 days. There was no change in the pattern or intensity of *CRX* expression in Smo^c- versus eGFP- infected retinal explants, indicating that Smo^c expression did not interfere with commitment to the photoreceptor fate in the uninfected cells. Furthermore, there was no contribution of cell death to this disrupted rhodopsin expression, since there were no significant dead cells in Smo^c-infected retinal explants. Considering that I did not see any disruption in rhodopsin expression at 7 days, my results indicate that the Smo^c-infected cells had an inhibitory effect on the maintenance of rhodopsin expression by 10 days. In addition, the location of Smo^c-infected cells in the retinal explants did not appear to matter, because there was no bias of the locations of gfp^+ cells, which were observed in the $rhodopsin^+$ and the $rhodopsin^-$ regions.

There is a considerable lag, between 5.5-6.5 days, between terminal cell cycle exit and rhodopsin expression in rod photoreceptors (32). Even in E18.5 retinal explants cultured for 7 days (equivalent to P7), rod photoreceptor differentiation is still not complete. Therefore, it is difficult to discern whether the Smo^c-infected cells inhibited rhodopsin

expression in rhodopsin$^-$ pre-rods or whether it had a negative effect on rhodpsin expression on cells that had initiated rhodopsin expression. Because cell survival in explants cultured for longer than 10 days was poor, it was not possible to determine if the negative effect of Smo^c on rhodopsin expression was permanent.

In many tissues, the long-range effects of Shh are direct, and most likely mediated by the formation of multimerized diffusible forms of Hh (74, 108). This soluble form of Shh can be isolated from chick limb buds, a biologically relevant source of Shh. In such tissues, s-ShhNp is thought to be freely diffusible and able to form a gradient to facilitate a long-range signalling (108). There are also several other examples where Shh induces the expression of 2nd diffusible signals to reach the long-range effects, such as TGFβ and FGF family members (75, 109). In my project, the cell-autonomous activation of the Hh signalling pathway was transduced by activating its receptor directly, no requirement for release and transport of the Hh signal. However, the decreased rhodopsin expression was detected in a large extent, not only in the Smo^c-infected cells. Thus, it is likely that the negative effects on rhodopsin expression could be mediated by the production of a diffusible signal from the Smo^c-infected cells. I do not know the identity of this signal, but there are several possible candidates that should be tested. Among the several molecules that have been shown to negatively influence photoreceptor differentiation in vitro, the Müller glia-derived LIF was inhibitory for rhodopsin expression in postmitotic "pre-rod" cells (40). Since Smo^c-expression promoted the proliferation of Müller glia, this observation raises the possibility that the inhibition on rhodopsin expression in the Smo^c-infected explants could be secondary to an increase in LIF production by the increased Müller glia in these explants. Thus, it

whether the effects of Smo^c expression on rod photoreceptor differentiatin could be inhibited by blocking LIF signalling.

References

1. Pei, Y.F., and J.A. Rhodin. 1970. The prenatal development of the mouse eye. *Anat Rec* 168:105-125.
2. Dowling JE. 1987. The retina-An approachable part of the brain. *harvard Univ. press, Cambridge, Massachusetts.*
3. Young, R.W. 1985. Cell proliferation during postnatal development of the retina in the mouse. *Dev. Brain. Res* 21:229-239.
4. Jeon CJ, S.E., Masland RH. 1998. The major cell populations of the mouse retina. *J Neurosci* 18:8936-8946.
5. Cepko, C.G., JA. Szeie, FG. Lin, J. 1997. in Molecular and Cellular Approaches to Neural Development. Oxford Univ. Press, New York.
6. Cepko, C.R., E. Austin, C. Golden, J. Fields-Berry, S and Lin, J. 1998. Lineage analysis using retroviral vectors. *methods*:393-406.
7. Cayouette, M., B.A. Barres, and M. Raff. 2003. Importance of intrinsic mechanisms in cell fate decisions in the developing rat retina. *Neuron* 40:897-904.
8. Reh, T.L., EM. 1998. Multipotential stem cells and progenitors in the vertebrate proliferation. *J. Neurobiol*:206-220.
9. Cepko, C.L., C.P. Austin, X. Yang, M. Alexiades, and D. Ezzeddine. 1996. Cell fate determination in the vertebrate retina. *Proc Natl Acad Sci U S A* 93:589-595.
10. Dyer, M.A. 2003. Regulation of proliferation, cell fate specification and differentiation by the homeodomain proteins Prox1, Six3, and Chx10 in the developing retina. *Cell Cycle* 2:350-357.
11. Levine, E.G., ES. 2004. Cell-intrinsic regulators of proliferation in vertebrate retinal progenitors. *Seminars in Cell & Developmental Biology*:63-74.

12. Livesey, F.J., and C.L. Cepko. 2001. Vertebrate neural cell-fate determination: lessons from the retina. *Nat Rev Neurosci* 2:109-118.

13. Cameron HA, H.T., McKay RD. 1998. Regulation of neurogenesis by growth factors and neurotransmitters. *J Neurobiol*:287-306.

14. Levine, E.F., S. Reh, TA. 2000. Soluble factors and the development of rod photoreceptors. *Cell. Mol. Life Sci*:224-234.

15. Megason, S.M., AP. 2002. A mitogen gradient of dorsal midline Wnts organizes growth in the CNS. *Development*:2087-2098.

16. Planas-Silva, M.D., and R.A. Weinberg. 1997. The restriction point and control of cell proliferation. *Curr Opin Cell Biol* 9:768-772.

17. Maanday, E.V.d.V., M. Vlaar, M. Feltkamp,C. O'Brien,J. van Roon,M. 1994. Developmental rescue of an embryonic-lethal mutation in the retinoblastoma gene in chimeric mice. *EMBO J*:4260-4268.

18. Robanus-Maanbag, E.D., M. van der Valk,M. Carrozza,ML. Jeanny, JC. Dannenberg, JH. 1998. p107 is a suppressor of retinoblastoma development in pRb-deficient mice. *Genes & development*:1599-1609.

19. Chen, D., I. Livne-bar, J.L. Vanderluit, R.S. Slack, M. Agochiya, and R. Bremner. 2004. Cell-specific effects of RB or RB/p107 loss on retinal development implicate an intrinsically death-resistant cell-of-origin in retinoblastoma. *Cancer Cell* 5:539-551.

20. Sicinski, P.D., Jl. Parker, SB. Fazeli,A Gardner, H. 1995. Cyclin D1 provides a link between development and oncogenesis in the retina and brease. *Cell*:621-630.

21. Ciemerych, M.K., AM. Sicinska, E. Kalaszczynska,I. Bronson, RT. Rowitch, DH. 2002. Development of mice expressing a single D-type cyclin. *Genes & development*:3277-3289.

22. Bernier, G.P., F. Zhou, X. Hollemann, T. Gruss, P. Pieler, T. 2000. Expanded retina territory by midbrain transformation upon overexpression of Six6(Optx2) in *Xenopus* embryos. *Mech Dev*:59-69.

23. Li, X.P., V. Liu,F. Rose, DW. Rosenfeld, MG. 2002. Tissue-specific regulation of retinal and pituitary precursor cell proliferation. *Science*:1180-1183.

24. Belecky-Adams, T., S. Tomarev, H.S. Li, L. Ploder, R.R. McInnes, O. Sundin, and R. Adler. 1997. Pax-6, Prox 1, and Chx10 homeobox gene expression correlates with phenotypic fate of retinal precursor cells. *Invest Ophthalmol Vis Sci* 38:1293-1303.

25. Green, E.S., JL. Levine, EM. 2003. Genetic rescue of cell number in a mouse model of microphthalmia: interactions between Chx10 and G1-phase cell cycle regulators. *Development*:539-552.

26. Lillien, L., and C. Cepko. 1992. Control of proliferation in the retina: temporal changes in responsiveness to FGF and TGF alpha. *Development* 115:253-266.

27. Anchan, R.M., T.A. Reh, J. Angello, A. Balliet, and M. Walker. 1991. EGF and TGF-alpha stimulate retinal neuroepithelial cell proliferation in vitro. *Neuron* 6:923-936.

28. Tropepe, V., B.L. Coles, B.J. Chiasson, D.J. Horsford, A.J. Elia, R.R. McInnes, and D. van der Kooy. 2000. Retinal stem cells in the adult mammalian eye. *Science* 287:2032-2036.

29. Fischer, A.J., and T.A. Reh. 2002. Exogenous growth factors stimulate the regeneration of ganglion cells in the chicken retina. *Dev Biol* 251:367-379.

30. Wang, Y.P., G. Dakubo, P. Howley, K.D. Campsall, C.J. Mazarolle, S.A. Shiga, P.M. Lewis, A.P. McMahon, and V.A. Wallace. 2002. Development of normal retinal organization depends on Sonic hedgehog signaling from ganglion cells. *Nat Neurosci* 5:831-832.

31. Jensen, A.M., and V.A. Wallace. 1997. Expression of Sonic hedgehog and its putative role as a precursor cell mitogen in the developing mouse retina. *Development* 124:363-371.

32. Morrow, E.M., M.J. Belliveau, and C.L. Cepko. 1998. Two phases of rod photoreceptor differentiation during rat retinal development. *J Neurosci* 18:3738-3748.

33. Rapaport, D.H., S.L. Patheal, and W.A. Harris. 2001. Cellular competence plays a role in photoreceptor differentiation in the developing Xenopus retina. *J Neurobiol* 49:129-141.

34. Belliveau, M.J., and C.L. Cepko. 1999. Extrinsic and intrinsic factors control the genesis of amacrine and cone cells in the rat retina. *Development* 126:555-566.

35. Belliveau, M.J., T.L. Young, and C.L. Cepko. 2000. Late retinal progenitor cells show intrinsic limitations in the production of cell types and the kinetics of opsin synthesis. *J Neurosci* 20:2247-2254.

36. Zhang, X.Y., XJ. 2001. Regulation of retinal ganglion cell production by Sonic hedgehog. *Development*:943-957.

37. Ezzeddine, Z.D., X. Yang, T. DeChiara, G. Yancopoulos, and C.L. Cepko. 1997. Postmitotic cells fated to become rod photoreceptors can be respecified by CNTF treatment of the retina. *Development* 124:1055-1067.

38. Furukawa, T., S. Mukherjee, Z.Z. Bao, E.M. Morrow, and C.L. Cepko. 2000. rax, Hes1, and notch1 promote the formation of Muller glia by postnatal retinal progenitor cells. *Neuron* 26:383-394.

39. Furukawa, T., E.M. Morrow, and C.L. Cepko. 1997. Crx, a novel otx-like homeobox gene, shows photoreceptor-specific expression and regulates photoreceptor differentiation. *Cell* 91:531-541.

40. Neophytou, C., A.B. Vernallis, A. Smith, and M.C. Raff. 1997. Muller-cell-derived leukaemia inhibitory factor arrests rod photoreceptor differentiation at a postmitotic pre-rod stage of development. *Development* 124:2345-2354.

41. Cao, W., W. Chen, R. Elias, and J.F. McGinnis. 2000. Recoverin negative photoreceptor cells. *J Neurosci Res* 60:195-201.

42. Sparrow, J.R., D. Hicks, and C.J. Barnstable. 1990. Cell commitment and differentiation in explants of embryonic rat neural retina. Comparison with the developmental potential of dissociated retina. *Brain Res Dev Brain Res* 51:69-84.

43. Watanabe, T., and M.C. Raff. 1990. Rod photoreceptor development in vitro: intrinsic properties of proliferating neuroepithelial cells change as development proceeds in the rat retina. *Neuron* 4:461-467.

44. Watanabe, T.R., MC. 1992. Diffusible rod-promoting signals in the developing rat retina. *Development*:899-906.

45. Kelley, M.W., J.K. Turner, and T.A. Reh. 1994. Retinoic acid promotes differentiation of photoreceptors in vitro. *Development* 120:2091-2102.

46. Altshuler, D., J.J. Lo Turco, J. Rush, and C. Cepko. 1993. Taurine promotes the differentiation of a vertebrate retinal cell type in vitro. *Development* 119:1317-1328.

47. Hicks, D., and Y. Courtois. 1992. Fibroblast growth factor stimulates photoreceptor differentiation in vitro. *J Neurosci* 12:2022-2033.

48. Hunter, D.D., M.D. Murphy, C.V. Olsson, and W.J. Brunken. 1992. S-laminin expression in adult and developing retinae: a potential cue for photoreceptor morphogenesis. *Neuron* 8:399-413.

49. Kirsch, M., S. Fuhrmann, A. Wiese, and H.D. Hofmann. 1996. CNTF exerts opposite effects on in vitro development of rat and chick photoreceptors. *Neuroreport* 7:697-700.

50. Nusslein-Volhard, C., and E. Wieschaus. 1980. Mutations affecting segment number and polarity in Drosophila. *Nature* 287:795-801.

51. Roelink. H, e.a. 1994. Floor plate and motor neuron induction by vhh-1, a vertebrate homolog of Hedgehog expressed by the notocord. *cell*:761-775.

52. Riddle. RD, J.R., Laufer. E.& Tavin. CJ. 1993. Sonic hedgehog mediates the polarizing activity of the ZPA. *Cell*:1401-1416.

53. Bitgood, M.J., and A.P. McMahon. 1995. Hedgehog and Bmp genes are coexpressed at many diverse sites of cell-cell interaction in the mouse embryo. *Dev Biol* 172:126-138.

54. Bitgood, M.J., L. Shen, and A.P. McMahon. 1996. Sertoli cell signaling by Desert hedgehog regulates the male germline. *Curr Biol* 6:298-304.

55. Yamada, T., S.L. Pfaff, T. Edlund, and T.M. Jessell. 1993. Control of cell pattern in the neural tube: motor neuron induction by diffusible factors from notochord and floor plate. *Cell* 73:673-686.

56. Fan, C.M., and M. Tessier-Lavigne. 1994. Patterning of mammalian somites by surface ectoderm and notochord: evidence for sclerotome induction by a hedgehog homolog. *Cell* 79:1175-1186.

57. Vaahtokari, A., T. Aberg, J. Jernvall, S. Keranen, and I. Thesleff. 1996. The enamel knot as a signaling center in the developing mouse tooth. *Mech Dev* 54:39-43.

58. Levin, M., S. Pagan, D.J. Roberts, J. Cooke, M.R. Kuehn, and C.J. Tabin. 1997. Left/right patterning signals and the independent regulation of different aspects of situs in the chick embryo. *Dev Biol* 189:57-67.

59. Lee, J.J., S.C. Ekker, D.P. von Kessler, J.A. Porter, B.I. Sun, and P.A. Beachy. 1994. Autoproteolysis in hedgehog protein biogenesis. *Science* 266:1528-1537.

60. Porter, J.A., D.P. von Kessler, S.C. Ekker, K.E. Young, J.J. Lee, K. Moses, and P.A. Beachy. 1995. The product of hedgehog autoproteolytic cleavage active in local and long-range signalling. *Nature* 374:363-366.

61. Porter, J.A., K.E. Young, and P.A. Beachy. 1996. Cholesterol modification of hedgehog signaling proteins in animal development. *Science* 274:255-259.

62. pepinsky, R., Zeng, C., Wen, D., Rayhorn,P., Baker, D., Williams, K., Bixler, S., Ambrose, C., Garber, E., Miatkowski, K.,. 1998. Identification of a palmitic acid-modified form of human Sonic hedgehog. *J.Biol. Chem.*:14037-14045.

63. Chamoun, Z., Mann, RK., Nellen, D., von Kessler, DP., Bellotto, M. 2001. Skinny hedgehog, an acyltransferase required for palmitoylation and activity of the hedgehog signal. *Science*:2080-2084.

64. Berthiaume, L. 2002. Insider information: how palmitoylation of Ras makes it a signaling double agent. *Sci STKE*:PE41.

65. Marigo, V., R.A. Davey, Y. Zuo, J.M. Cunningham, and C.J. Tabin. 1996. Biochemical evidence that patched is the Hedgehog receptor. *Nature* 384:176-179.

66. Taipale, J., M.K. Cooper, T. Maiti, and P.A. Beachy. 2002. Patched acts catalytically to suppress the activity of Smoothened. *Nature* 418:892-897.

67. Zhang, X.R.-S., M. McMahon, AP. 2001. Smoothened mutants reveal redundant roles for Shh and Inn signaling including regulation of L/R asymmetry the mouse node. *Cell*:781-792.

68. Lee, J.P., K. Censullo, P. Altaba, A. 1997. Gli1 is a target of sonic hedgehog that induces ventral neural-tube development. *Development*:2537-2552.

69. Marigo, V.J., R. Vortkamp,A. Tabin, C. 1996. Sonic hedghog differentially regulates expressin of *Gli1* and *Gli3* during limb development. *Dev. Biol.*:273-283.

70. Zhu, Y., R.M. James, A. Peter, C. Lomas, F. Cheung, D.J. Harrison, and S.A. Bader. 2004. Functional Smoothened is required for expression of GLI3 in colorectal carcinoma cells. *Cancer Lett* 207:205-214.

71. Hammerschmidt, M., A. Brook, and A.P. McMahon. 1997. The world according to hedgehog. *Trends Genet* 13:14-21.

72. Gutierrez-Frias C, S.R., Hernandez-Lopez C, Cejalvo T, Crompton T, Zapata AG, Varas A, Vicente A. 2004. Sonic hedgehog regulates early human thymocyte differentiation by counteracting the IL-7-induced development of CD34+ precursor cells. *J Immunol* 173:5046-5053.

73. Orentas, D.H., J. Dyer, K. Miller, R. 1999. Sonic hedgehog signalling is required during the appearance of spinal cord oligodendrocyte precursors. *Development*:2419-2429.

74. Briscoe J, C.Y., Jessell TM, Struhl G. 2001. A hedgehog-insensitive form of patched provides evidence for direct long-range morphogen activity of sonic hedgehog in the neural tube. *Mol. Cell.*:1279-1291.

75. Drossopoulou, G.L., K. Sanz-Ezquerro, J. Nikbakht, N. McMahon, A, Hofman, C. Tickle, C. 2000. A model for anteroposterior patterning of the vertebrate limb based on sequential long- and short-range Shh signalling and Bmp signalling. *Development*:1337-1348.

76. Placzek, M. 1995. The role of the notochord and floor plate in inductive interactions. *Curr Opin Genet. Dev*:499-506.

77. Wallace, V.A., and M.C. Raff. 1999. A role for Sonic hedgehog in axon-to-astrocyte signalling in the rodent optic nerve. *Development* 126:2901-2909.

78. Levine, E.R., H. Turner, J. Reh, TA. 1997. Sonic hedgehog promotes rod photoreceptor differentiation in mammalian retinal cells in vitro. *J. Neurosci*:6277-6288.

79. Dakubo, G.D., and V.A. Wallace. 2004. Hedgehogs and retinal ganglion cells: organizers of the mammalian retina. *Neuroreport* 15:479-482.

80. Neumann, C.N.-V., C. 2000. Patterning of the zebrafish retina by a wave of sonic hedgehog activity. *Science*:2137-2139.

81. Xie, J., M. Murone, S.M. Luoh, A. Ryan, Q. Gu, C. Zhang, J.M. Bonifas, C.W. Lam, M. Hynes, A. Goddard, A. Rosenthal, E.H. Epstein, Jr., and F.J. de Sauvage. 1998. Activating Smoothened mutations in sporadic basal-cell carcinoma. *Nature* 391:90-92.

82. Hynes, M., W. Ye, K. Wang, D. Stone, M. Murone, F. Sauvage, and A. Rosenthal. 2000. The seven-transmembrane receptor smoothened cell-autonomously induces multiple ventral cell types. *Nat Neurosci* 3:41-46.

83. Hatakeyama J, K.R. 2002. Retrovirus-mediated gene transfer to retinal explants. *Methods*:387-395.

84. Weiss, R. 1984. Retroviruses linked with AIDS. *Nature* 309:12-13.

85. Roe, T.R., TC. Yu, G and Browns, PO. 1993. Integration of murine leukemia virus DNA depends on mitosis. *EMBO J*:2099-2108.

86. Bender, M.P., TD. Gelinas, RE. Miller, AD. 1987. Evidence that the packaging signal of Moloney murine leukemia virus extends into the gag region. *J. Virol*:1639-1646.

87. Ausubel, F.B., R. Kingston, RE. Moore, DD. Seidman, JG. Smith, JA. and Struhul, K. 1997. current protocol in Molecular Biology.

88. Soneoka, Y.C., PM. Ramsdale, EE. Griffiths, JC. Ramano, G. Kingsman, SM. Kingsman, AJ. 1995. A transient three-plasmid expression system for the production of high titer retroviral vectors. *Nucleic Acids Res*:628-633.

89. Turner, D.L., E.Y. Snyder, and C.L. Cepko. 1990. Lineage-independent determination of cell type in the embryonic mouse retina. *Neuron* 4:833-845.

90. J. Sambrook, E.F.F., T. Maniatis. 1989. Molecular cloning. cold spring harbor laboratory press.

91. Wendy J Ingram, C.A.W., Sean M Grimmond, Alistair R Forrest and, and B.J. Wainwright. 2002. Novel genes regulated by Sonic Hedgehog in pluripotent mesenchymal cells. *oncogene* 21:8196-8205.

92. Sanes JR, R.J., Nicolas JF. 1986. Use of a recombinant retrovirus to study post-implantation cell lineage in mouse embryos. *EMBO J.* 5:3133-3141.

93. Crabb, J.W., V.P. Gaur, G.G. Garwin, S.V. Marx, C. Chapline, C.M. Johnson, and J.C. Saari. 1991. Topological and epitope mapping of the cellular retinaldehyde-binding protein from retina. *J Biol Chem* 266:16674-16683.

94. Laird, D.W., and R.S. Molday. 1988. Evidence against the role of rhodopsin in rod outer segment binding to RPE cells. *Invest Ophthalmol Vis Sci* 29:419-428.

95. Chen, C.K. 2002. Recoverin and rhodopsin kinase. *Adv Exp Med Biol* 514:101-107.

96. Nishina, S., S. Kohsaka, Y. Yamaguchi, H. Handa, A. Kawakami, H. Fujisawa, and N. Azuma. 1999. PAX6 expression in the developing human eye. *Br J Ophthalmol* 83:723-727.

97. Greferath, U., U. Grunert, and H. Wassle. 1990. Rod bipolar cells in the mammalian retina show protein kinase C-like immunoreactivity. *J Comp Neurol* 301:433-442.

98. Fisher, L.J. 1997. Neural Precursor Cells: Applications for the Study and Repair of the Central Nervous System. *Neurobiology of Disease*:1-22.

99. Raff, M. 1989. Glial cell diversification in the rat optic nerve. *Science*:1450-1455.

100. Zhang, J., A. Rosenthal, F.J. de Sauvage, and R.A. Shivdasani. 2001. Downregulation of Hedgehog signaling is required for organogenesis of the small intestine in Xenopus. *Dev Biol* 229:188-202.

101. Kenney, A.R., DH. 2000. Sonic hedgehog promotes G(1) cyclin expression and sustained cell cyclin progression in mammalian neuronal precursor. *Mol. Cell. Biol*:9055-9067.

102. Fan, H.K., PA. 1999. Sonic hedgehog opposes epithelial cell cycle arrest. *J. Cell Biol.*:71-76.

103. Stenkamp, D.F., RA. Prabhudesai, SN. Raymond, PA. 2000. Function for hedgehog genes in zebrafish retinal development. *Dev. Biol.*:238-252.

104. Tomita, K., M. Ishibashi, K. Nakahara, S.L. Ang, S. Nakanishi, F. Guillemot, and R. Kageyama. 1996. Mammalian hairy and Enhancer of split homolog 1 regulates differentiation of retinal neurons and is essential for eye morphogenesis. *Neuron* 16:723-734.

105. Willbold, E., and P.G. Layer. 1998. Muller glia cells and their possible roles during retina differentiation in vivo and in vitro. *Histol Histopathol* 13:531-552.

106. Shkumatava A, F.S., Muller F, Strahle U, Neumann CJ. 2004. Sonic hedgehog, secreted by amacrine cells, acts as a short-range signal to direct differentiation and lamination in the zebrafish retina. *Development*:3849-3858.

107. Jarov, A., K.P. Williams, L.E. Ling, V.E. Koteliansky, J.L. Duband, and C. Fournier-Thibault. 2003. A dual role for Sonic hedgehog in regulating adhesion and differentiation of neuroepithelial cells. *Dev Biol* 261:520-536.

108. Fan, C.M., J.A. Porter, C. Chiang, D.T. Chang, P.A. Beachy, and M. Tessier-Lavigne. 1995. Long-range sclerotome induction by sonic hedgehog: direct role of the amino-terminal cleavage product and modulation by the cyclic AMP signaling pathway. *Cell* 81:457-465.

109. Roussa, E., L.M. Farkas, and K. Krieglstein. 2004. TGF-beta promotes survival on mesencephalic dopaminergic neurons in cooperation with Shh and FGF-8. *Neurobiol Dis* 16:300-310.

Appendices

Appendix A: RNA purification and RT-PCR reaction

Purify RNA from Tri-reagents (Sigma, T-9424)

1. Put 1 ml of tri-reagent solution to the cell culture dish and then homologize the cells.
2. Add 0.2 ml of chloroform, shake 15 seconds and stand at RT for 2-15 min.
3. Spin 12,000g at 4°C for 15 min.
4. Transfer the aqueous phase to a new tube and add 0.5 ml of iso-propanol. Mix well and stand at RT for 2-15 min; and spin at 12,000g for 15 min.
5. Harvest the pellet and add 1 ml of 75% ethanol. Vortex well and centrifuge at 12,000g for 10 min at 4°C.

Reverse Transcription reaction (Invitrogen, ThermoScript™ RT-PCR system, #11146-016)

In a 20 μl RT-PCR reaction system, first make the following solution A:

Random Hexamers (50 ng/μl)	1 μl
dNTP (10mM)	1μl
RNA (purified according to the protocol above)	2 μg
DEPC-H_2O	
Make volume at 12 μl	

→ mix, 65°C, 5 min → put on ice.

Add the following solution B to the solution A:

5 x first-strand buffer	4 μl
0.1M DTT	2 μl
RNase OUT (40U/μl)	1 μl

→ mix, 37°C, 2 min.

At last, add SuperScript Rtase (15U/μl) 1 μl

→ mix, 25°C, 10min →37°C , 50min →75°C, 15min.

PCR reaction

Follow the standard protocol in Molecular cloning: A laboratory manual, 2nd edition. Cold spring harbour laboratory press. 1989

Appendix B.

Table 1. Primary antibodies used in the immunohistochemistry and nulcei labeling

primary antibody	targets	host	dilution	source	Cat number
anti-GFP	gfp-positive cells	rabbit	1:1000	Molecular Probe	A-11122
	gfp-positive cells	mouse	1:100	Molecular Probe	A-11120
anti-rhodopsin	rods (rhodopsin+)	mouse	1:3	Developmental studies hybridoma bank	
anti-recoverin	rods, cones, midget bipolar cells	rabbit	1:1000	Chemicon International	AB 5585
anti-CRALBP	Müller cells	rabbit	1:2000	the lab of J.C.Saari, Univ. of Washingt	206-543-5792
anti-Pax6	amacrine cells, precursor cells, ganglion cells, horizontal cells	mouse	1:3	Developmental studies hybridoma bank	
anti-PKC	bipolar cells	mouse	1:100	BD Biosciences	554207
anti-nestin	precursors, Müller cells	mouse	1:100	StemCell Technologies	1418
anti-BrdU	BrdU-positive cells	mouse	1:100	Becton Dickinson	347580

Appendix C

Table 2. Secondary antibodies used in immunohistochemistry

secondary antibody	host	dilution	source	Cat number
AlexFluor 488	goat anti mouse	1:500	Molecular Probe	A 11029
AlexFluor 488	goat anti rabbit	1:500	Molecular Probe	A 11034
Cy3-conjugated Affini Pure	goat anti mouse	1:500	Jackson ImmunoResearch	115-005-003
Cy3-conjugated Affini Pure	goat anti rabbit	1:500	Jackson ImmunoResearch	111-166-003

Appendix D

Hybridization buffer
1x salt
50% deionized formamide
10% dextran sulphate
1 mg/ml rRNA
1x Denhardt's

*Pre-warm at 65 °C before adding probe.
*Make up volume with Baxter water.

10x Salt (1L)

NaCl		114g
Tris HCl (pH 7.5)		14.04g
Tris base		1.34g
Na $H_2PO_4 \bullet 2H_2O$		7.8g
$Na_2 HPO_4$		7.1g
0.5M EDTA (made in DEPC-treated water)	100 ml	

*Make up volume with DEPC-treated water

100x Denhardt's (100 ml)

2% w/v BSA	2g
2% w/v Ficoll™ (400)	2g
2% w/v polyvinyl pyrolidone	2g

*Make up volume with Baxter water

rRNA
*Dissolve yeast rRNA (BM) in DEPC-treated water at 10 mg/ml.

Appendix E

Staining buffer
100mM NaCl
50mM $MgCl_2$
100mM Tris (pH 9-9.5)
0.1% Tween-20

To make 70 ml staining buffer in the last step of staining: take 66.5 ml staining buffer without Tween-20 and $MgCl_2$ and add 10% polyvinyl alcohol (PVA). Heat up to 80 °C to dissolve with constant stirring. Once dissolved and cooled down to room temperature, adding 50mM of $MgCl_2$ and 0.1% Tween-20 and continue stirring. Shield from light and add 4.5 µg/ml of NBT and 3.5 µg/ml of BCIP. Add this staining buffer to sections immediately.

Curriculum Vitae

Name: Chuan Yu
Birthday: Nov 9th, 1975
Birth place: Dalian city, Liaoning Province, P.R.China
Citizenship: P.R.China

Educations

1. Sept 2002 --- present M.Sc. candidate
Dept. of Biochemistry, Microbiology and Immunology, Univ. of Ottawa, Canada

2. Sept 1999 --- Aug 2002 M.Sc.
Division of Molecular Biology, Shanghai Institutes for Life Science,
Chinese Academy of Sciences. P.R.China

3. Sept 1994 --- Jul 1998 B.Sc.
Dept. of Molecular and Developmental Biology, School of Life Science,
Wuhan Univ. P.R.China

Awards

1. Jan 2003—Dec 2004, training award for graduate students from Stem Cell Network, Canada.
2. 2001, "DI AO" Scholarship from Chinese Academy of Sciences.

Publications and academic meeting presentations

1. Yu C, Wallace V. Cell autonomous effects of the Hh signalling pathway in the murine retina development. Poster presentation. Stem Cell Network Annual General Meeting in Montreal, Canada, Nov 2004
2. Yu C, Wallace V. Cell autonomous effects of the Hh signalling pathway in the murine retina development. Poster presentation. Stem Cell Network Annual General Meeting in Vancouver, Canada, Sept 2003.
3. Yu C, Meng X, Zhang S, Zhao G, Hu L, Kong X. A 3-nucleotide deletion in the polypyrimidine tract of intron 7 of the DFNA5 gene causes nonsyndromic hearing impairment in a Chinese family. *Genomics*. 2003 Nov; 82(5): 575-9
4. Bu L, Yan S, Jin M, Jin Y, Yu C, Xiao S, Xie Q, Hu L, Xie Y, Solitang Y, Liu J, Zhao G, Kong X. The gamma S-crystallin gene is mutated in autosomal recessive cataract in mouse. Genomics. 2002 Jul; 80(1): 38-44.
5. Xiao S, Yu C, Chou X et al. Dentinogenesis imperfecta 1 with or without progressive hearing loss is associated with distinct mutations in DSPP. *Nat Genet*. 2001 Feb; 27(2): 201-4.